Structure-property relationship of 4-substituted-spirobifluorenes as hosts for phosphorescent organic light emitting diodes: an overview

Cyril Poriel, Joëlle Rault-Berthelot

Structure-Properties Relationship of 4-Substituted-Spirobifluorenes as Hosts for Phosphorescent Organic Light Emitting Diodes : An overview

Cyril Poriel,[†*] Joëlle Rault-Berthelot[†]

[†] Université de Rennes 1-UMR CNRS 6226 "Institut des Sciences Chimiques de Rennes"- MaCSE group, Bat 10C, Campus de Beaulieu - 35042 Rennes cedex, France

KEYWORDS. 4-substituted–spirobifluorenes, spiro compounds, Phosphorescent OLEDs, Host Material, Pure Hydrocarbons, triplet energy, organic electronics

Abstract

The aim of the present review is to report the state of the art of an emerging family of molecules, namely the 4-substituted spirobifluorenes (SBFs). The syntheses, physico-chemical and photophysical properties and applications as host in Phosphorescent Organic Light-Emitting diodes (PhOLEDs) are described through a structure-properties relationship approach. If the substitution in position 2 of a SBF core has widely been developed, the substitution in position 4 is very recent (less than that 10 years) and still need to be explored.

1. Introduction

Spiro-configured compounds constitute one of the most important class of Organic Semi-Conductors (OSCs).[1,2] In such compouds, at least two molecular π-systems with equal or different functions (emission, charge transport) are connected via a shared sp^3-hybridized atom. Such an architecture has several benefits due to the perpendicular arrangement of the π-systems and the resulting spiro-configured OSCs present many appealing properties such as high thermal/morphological and emission colour stability, which are key properties for Organic Light-Emitting Diodes (OLED) applications.[1-4]
Since the discovery of the 'spiro-concept' introduced in the nineties by Salbeck et al., 9,9'spirobifluorene (**SBF**), which is constituted by the orthogonal junction of two fluorenyl cores via a spiro carbon, has become a central scaffold in organic electronics.[1, 2] Indeed, **SBF** is a key building block in the design of blue emitting fluorophores or host materials for blue OLEDs, which are still the weakest link of the technology.[5] The SBF fragment is nevertheless not only used in the OLED technology but is also a key fragment in Organic Photovoltaic. Indeed, 2,2',7,7'-Tetrakis[N,N-di(4-methoxyphenyl)amino]-9,9'-spirobifluorene (Spiro-OMeTAD) is the prevalently used hole transporting material in solid-state dye-sensitized solar cells and, more recently in perovskite-absorber solar cells.[6, 7]
From a more fundamental point of view, the orthogonal configuration induced by the spiro carbon also allows to design shape persistent molecules with specific arrangements, which in turn has peculiar electronic consequences.[3, 4, 8-15] In addition, the application field of the SBF scaffold is not only restricted to electronics and SBF has also found many other appealing applications as chiral ligand,[16-19] electropolymerizable building block,[20-26] homogeneous[27] and heterogeneous[23-25, 28, 29] catalysts or as building unit in coordination polymers,[30-32] clearly showing the versatility of this fragment.

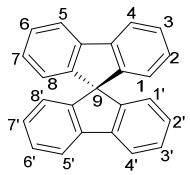

Figure 1. Nomenclature of the 9,9'-Spirobifluorene (**SBF**)

Sixteen positions of substitutions are available on the SBF backbone, eight on each fluorene unit (figure 1). In terms of nomenclature, the bridged carbon atom also called spiro carbon is the carbon

numbered 9 (or 9,9' in **SBF**) and the eight other carbon atoms are numbered from 1 to 8 and from 1' to 8' for each fluorene. In this review, we will only focus on the mono-substitution of the SBF derivatives. Thus, 2-substituted SBFs remain undoubtedly the most developed class of SBF-based polymers and oligomers.[2] The *para* linkage between the pendant substituent in position 2 and the constituted phenyl ring of the fluorene ensures a good delocalization of π-electrons, essential to develop efficient fluorophores.[2] However, in recent years the growing necessity to design efficient host materials for blue PhOLED has led to a huge demand of new generations of SBF based materials with wide band gap (*ca* 4 eV) and hence a restricted π-conjugation. Indeed, to obtain a very high triplet energy (E_T), key requirement in the design of host materials for blue PhOLEDs, it is mandatory to restrict the π-electrons delocalization within the OSC. To date, many successful design strategies, briefly exposed below, have been developed to disrupt the π-conjugation. First, it is known that electronic coupling through a *meta* linkage is inherently weaker than through a *para* one[3, 4, 33-37] and this strategy has often been used to connect a hole transporting and an electron transporting unit in a host material.[38-43] This *meta* linkage avoids strong electronic coupling between the two molecular fragments and hence keeps a high E_T. Using an insulating heteroatom is also an efficient strategy to obtain high E_T materials with short π-conjugated pathway. Thus, silicium (silane),[44-49] and phosphoryl group (P=O),[40, 44, 47, 50-53] may act as an effective breaking point of the π-conjugation between the main core of the molecule and the outer groups linked to the heteroatom (phenyl for example in the case of the efficient electron transporting diphenylphosphine oxide unit). More recently, another efficient molecular design based on a π-conjugation breaking induced by an insulating spiro bridge (Called Donor-Spiro-Acceptor design) has been also successfully introduced in literature.[46, 54-63] Finally, another approach widely developed in literature consists to introduce a steric congestion within the dye in order to hinder the planarization between two connected π-systems, which in turn breaks the π-conjugation between them.[64-66] This 'steric hindrance' strategy is most of the time performed through the incorporation of a sterically hindered *ortho* linkage[65, 67, 68] efficiently leading to a π-conjugation restriction. This last strategy is the basis of *ortho* linked SBFs (substitution in position 4)[68-71] which will be developed in this review. 4-substituted SBFs as host for PhOLEDs have started to appear in the literature less than 10 years ago and the SBF scaffold substituted in position 4 is undoubtedly a promising core for such applications. Through a structure properties relationship approach, the aim of the present review is to report the state of the art of this emerging family of molecules regarding synthesis, physico-chemical and photophysical properties and applications as host in PhOLEDs.

2. General synthesis of 4-Substituted SBFs

All the dyes investigated in this review have been synthesized from the 4-bromo-9,9'-spirobifluorene (**4-Br-SBF**) platform (Figure 2). This platform is undoubtedly the cornerstone of all the 4-substituted SBFs reported to date. Indeed, incorporation of a molecular fragment in position 4 of a SBF is more complicated than in position 2 as the direct electrophilic substitution of **SBF** does not occur on the C4 position of SBF but specifically on the C2 position.[2, 29] Thus, the direct incorporation of a fragment in C4 via an electrophilic aromatic substitution is not possible.

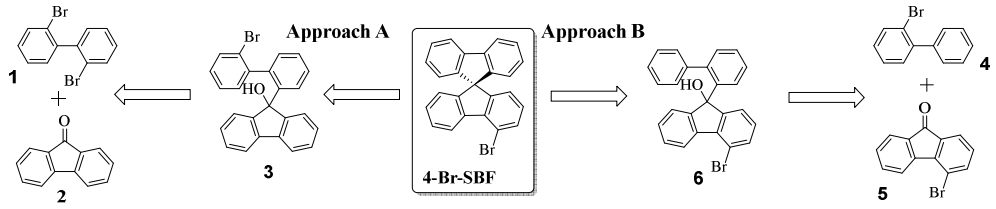

Figure 2. Retrosynthetic analyses of **4-Br-SBF** (Approaches A[70] and B[71])

First described in 1930,[72] **SBF** is obtained in a two-step route from 2-halogenobiphenyl (such as 2-bromo-biphenyl **4**) and 9-fluorenone **2** through a metal-halogen exchange reaction followed by an intramolecular cyclization of the resulting fluorenol to form the spiro carbon. The synthesis of the **4-Br-SBF** platform is based on the introduction of the bromine atom before this key cyclization step. Two

different approaches depicted in Figures 3 and 4 have been reported and are based on the introduction of the bromine atom either on the nucleophile (biphenyl **1**, Approach A-Figure 2) or on the electrophile (fluorenone **5**, Approach B-Figure 2).

The first rational synthesis of **4-Br-SBF** has been developed by the group of Ma in 2009 following the approach A[70] (Figure 2). In this approach (Figure 3), a mono lithium-halogen exchange of 2,2'-dibromobiphenyl **1** is performed in the presence of n-BuLi followed by the immediate trapping of the corresponding lithiated intermediate with 9-fluorenone **2**. The intramolecular electrophilic ring closure of the corresponding fluorenol **3** (not isolated), in acidic media, further provides **4-Br-SBF**. This efficient synthetic pathway allows obtaining **4-Br-SBF** with 83 % yield in two steps. This key platform or its pinacol analogue 4-(9,9'-spirobi[fluoren]-4-yl)-4,4,5,5-tetramethyl-1,3,2-dioxaborolane (**4-Pin-SBF**), synthesized with n-BuLi and pinacol borane from **4-Br-SBF** (Figure 3), will be then used to construct various 4-substituted SBFs through Pd catalysed reactions (see below).

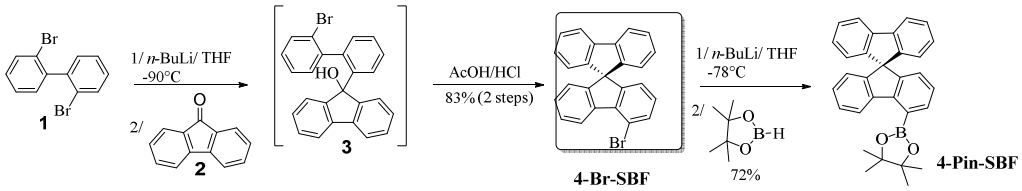

Figure 3. Synthesis of **4-Br-SBF** – Approach A[70]

The second approach towards **4-Br-SBF** (Approach B[71], Figure 2) reported in 2015 consists to fix the bromine atom on the fluorenone core (electrophile) prior to the final cyclisation. This route (Figure 4) involves the synthesis of a key building block: 4-bromo-9-fluorenone **5**, which is obtained by a Miyaura-Suzuki cross-coupling between phenylboronic acid **7** possessing an ethylcarboxylate group in position 2 and 2-bromoiodobenzene **8**. The selective cross-coupling reaction proceeds with 65% yield leading to the biphenyl **9** possessing on one ring the ethylcarboxylate and on the other a bromine atom. The intramolecular electrophilic aromatic substitution in acidic media (methanesulfonic acid: MsOH) leads to the formation of **5** with 95 % yield. The coupling of **5** with 2-lithiated biphenyl further provides the fluorenol **6** not isolated and involved in an intramolecular ring closure to give **4-Br-SBF** with high yield (75 % over the last three steps). The overall yield of the approach B, *ie* 46%, is lower than that of the approach A (83%),[70] but uses as key intermediate the versatile 4-bromo-fluorenone **5**. This molecule can be a useful building block to synthesize other families of OSCs constructed on the 4-fluorene scaffold such as dicyanovinylene,[73, 74] spiroxanthene,[75, 76] spirothioxanthene,[77] spirophenylacridine,[60, 61] spiroindoloacridine[63] and quinolinophenothiazine[62] derivatives.

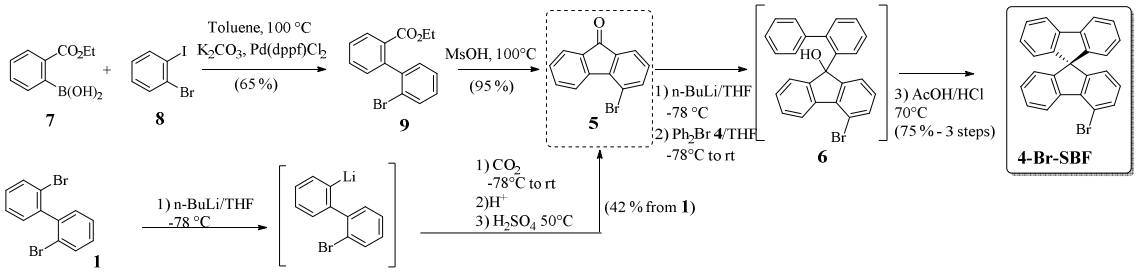

Figure 4. Synthesis of **4-Br-SBF** –Approach B

Fluorenone **5** has also been synthesized by Ma et al. using a different route (Figure 4, bottom).[69] Thus, **1** was treated with 1 equivalent of n-BuLi and then reacted with carbon dioxide to form the corresponding carboxylic acid further involved in an electrophilic cyclisation to provide **5** with 42 % yield.

In conclusion, all the dyes further reported herein have been synthesized from the key **4-Br-SBF** or its pinacol analogue **4-Pin-SBF**. These different cross-coupling reactions will be briefly developed in each part below.

3. Origin of the π-conjugation breaking

4-substituted SBFs belong to the new generation of SBFs, whereas 2-substituted SBFs can be seen as the 'first generation' of SBFs. The development of OSCs based on the 4-substituted SBFs has started with the development of the PhOLED technology and the need of organic host materials with high E_T. Indeed, in order to obtain a very high E_T, the π-electrons delocalization within the OSC should absolutely be restricted. Determining the origin of the π-conjugation disruption found in 4-substituted SBFs is the first important question to address herein.

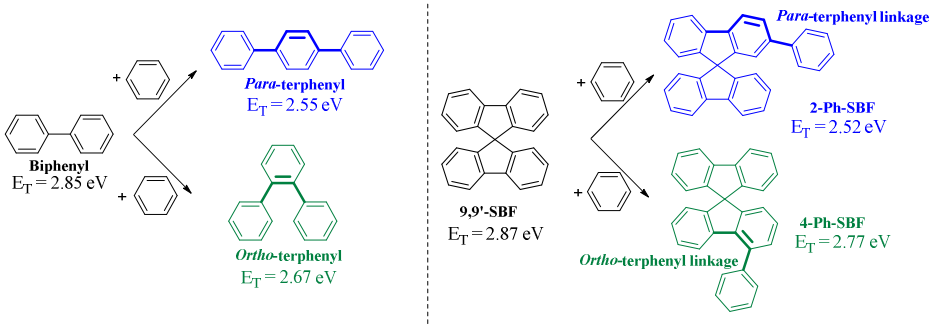

Figure 5. Biphenyl, *para*- and *ortho*-terphenyl (left) and **9,9'-SBF**, **2-Ph-SBF** and **4-Ph-SBF** (right) and their E_T.

In a 4-substituted SBF, the pending substituent is in *ortho* position of the biphenyl linkage (Figure 5-right) whereas in 2-SBF, the pending substituent is in *para* position. This feature is of great importance as very often an *ortho* linkage leads to a strong steric hindrance, which in turn can break the conjugation.[3, 36, 68, 78, 79] This feature can be exemplified with the terphenyl molecules possessing either a *para* or an *ortho* linkage (figure 5, left).[3, 36] First, we need to mention that biphenyl has an E_T of 2.85 eV.[80] Adding one phenyl unit either in *ortho* or in *para* position reduced this E_T due to the π-conjugation extension, however not with the same amplitude. Indeed, in the *para*-terphenyl, the conjugation is maximized due to the *para* linkages and the E_T is strongly decreased to 2.55 eV. In the *ortho*-terphenyl core, the *ortho* linkages lead to a strong steric hindrance, which maintains the E_T at 2.67 eV, higher than that of the *para*-terphenyl (figure 5, left).[3, 80]

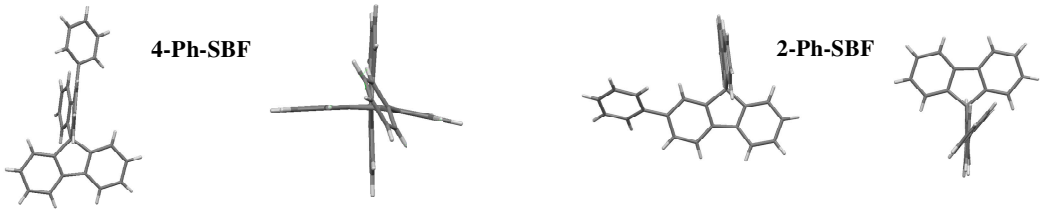

Figure 6. Molecular structure of **4-Ph-SBF** (left) and of **2-Ph-SBF** (right) (The asymmetric unit of both compounds contains two independent molecules, only one molecule is presented here for clarity)[81, 82]

As 4- and 2-substituted SBFs are respectively built on an *ortho*- and *para*-terphenyl backbone, similar properties evolution is expected. From a structural point of view, the main difference between 4-substituted-SBFs and 2-substituted-SBFs is found in the angle formed between the pendant substituent and its attached fluorene moiety. We will analyse this feature all along this review and particularly in this part through a representative example: the structural comparison of 4-phenyl-spirobifluorene (**4-Ph-SBF**)[81] and its regioisomer 2-phenyl-spirobifluorene (**2-Ph-SBF**) (Figure 6).[82] These two molecules are both constituted of a SBF core substituted by a phenyl ring either in position 4 for **4-Ph-SBF** or in position 2 for **2-Ph-SBF**. In **2-Ph-SBF**, the dihedral angle between the mean plane of the pendant phenyl ring and that of its attached phenyl ring of the fluorene has been reported at 37.4°.[82] This angle, characteristic of a non-encumbered phenyl/fluorene *para* linkage,[83] maximises the conjugation between the two fragments. In its regioisomer, **4-Ph-SBF**, the fluorene/phenyl dihedral angle is reported at 51.2° in molecule 1 and at 56.6° in molecule 2 (**4-Ph-SBF** indeed possesses an asymmetric unit containing two molecules 1 and 2, only the molecule 1 is presented in figure 6 for clarity purpose) being hence impressively larger than that of **2-Ph-SBF**. This structural feature has been

assigned by the authors to the steric interaction between the hydrogen atoms in *ortho* position of the pendant phenyl ring and those of the fluorenyl core[81] and is at the origin of the π-conjugation breaking observed in all 4-substituted SBFs.

Another structural feature is detected by the authors for **4-Ph-SBF** that is the intense deformation of the substituted fluorenyl core (this structural particularity will be also pointed for other 4-substituted SBFs as outlined below). Indeed, a dihedral angle as high as 12.7° is measured between the phenyl units of the substituted-fluorenyl core (Figure 6, left). Such structural deformation is more pronounced than that observed for the regioisomer **2-Ph-SBF** (deformation of ca 7.1°) and for **SBF** (1.2° and 4.2°).[81, 84] The deformation of the substituted fluorene in **4-Ph-SBF** has been assigned to intermolecular packings, which can induce a folding of the fluorenyl core. Thus, the *ortho* linkage found in 4-substituted SBFs has strong structural consequences, which will have important electronic repercussions. All the dyes, which will be described in the following of this review, present a large dihedral angle between the fluorene and its substituent in C4. However, we will see that this angle can be modulated depending of the nature of the substituent borne by the fluorene (see part 5).

4. Pure hydrocarbons (PHC) based on a 4-substituted SBF scaffold

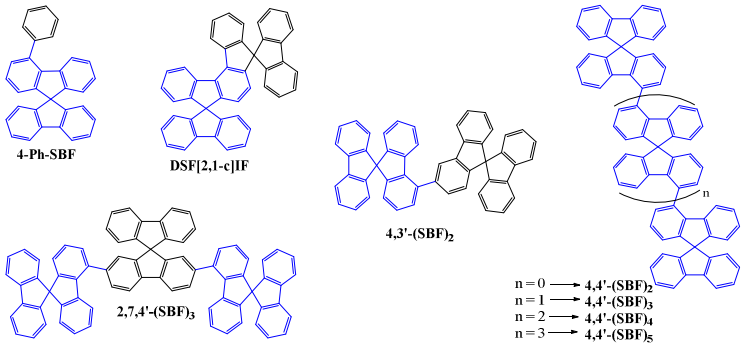

Figure 7: Pure hydrocarbon (PHC) derivatives based on a 4-substituted SBF scaffold

In order to obtain high-efficiency PhOLEDs, a good charge balance is necessary in the host and many different building blocks have been used for this purpose such as indolocarbazole,[85] phenylacridine,[60, 61, 86] indoloacridine,[63] phosphine oxide,[40, 53, 56] pyridine, benzimidazole[68] among others. However, it has been shown that the C-C bond is significantly stronger than the C-S, C-P or C-N bonds.[87] This molecular stability of pure hydrocarbons (PHC) renders them highly attractive and designing such materials for PhOLED applications is an active research field worldwide. In this part, we will review the PHCs constructed on a 4-substituted SBF scaffold (Figure 7) and will compare their properties with those of some of their regioisomers substituted in position 2 (Figure 8).

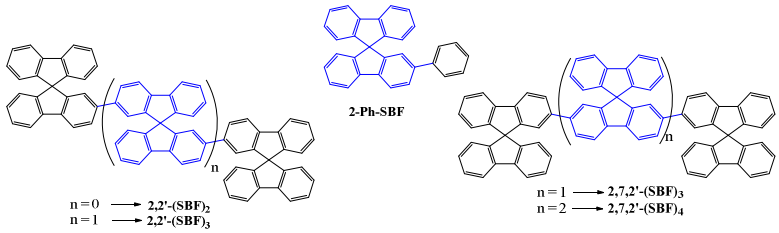

Figure 8: Pure hydrocarbon (PHC) derivatives based on a 2-substituted SBF scaffold

Synthesis

All the PHC molecules reported herein[69-71, 81, 88-90] have been synthesized from Suzuki couplings involving **4-Br-SBF** or its pinacol analogue **4-Pin-SBF** as starting materials. The syntheses of the 2-substituted SBFs, **2,7,2'-(SBF)$_3$**, **2,7,2'-(SBF)$_4$**[90] **2,2'-(SBF)$_3$**, **2,2'-(SBF)$_2$**[89] and **2-Ph-SBF**[71] will not be described.

Thus, **4-Ph-SBF** has been synthesized by the coupling of **4-Br-SBF** and phenylboronic acid through classical Suzuki conditions ($Pd(dppf)Cl_2/K_2CO_3$/DMF) with 91% yield, Figure 9. Similarly, oligo-SBFs **4,3'-(SBF)$_2$**, **2,7,4'-(SBF)$_3$** and **4,4'-(SBF)$_2$** have been synthesized from the coupling of **4-Br-SBF** with respectively spirobifluorene-3-boronic acid (**3-B(OH)$_2$-SBF**), 2,7-dibromo-spirobifluorene (**2,7-Br$_2$-SBF**) and **4-Pin-SBF** in good yields (81, 81 and 72 % *resp.*).

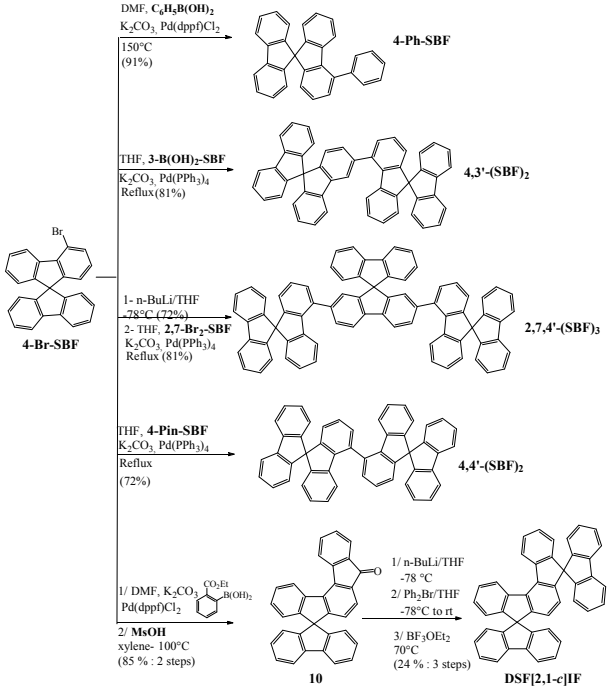

Figure 9. Synthesis of **4-Ph-SBF**, **4,3'-(SBF)$_2$**, **2,7,4'-(SBF)$_3$**, **4,4'-(SBF)$_2$**, **DSF[2,1-*c*]IF** from **4-Br-SBF**

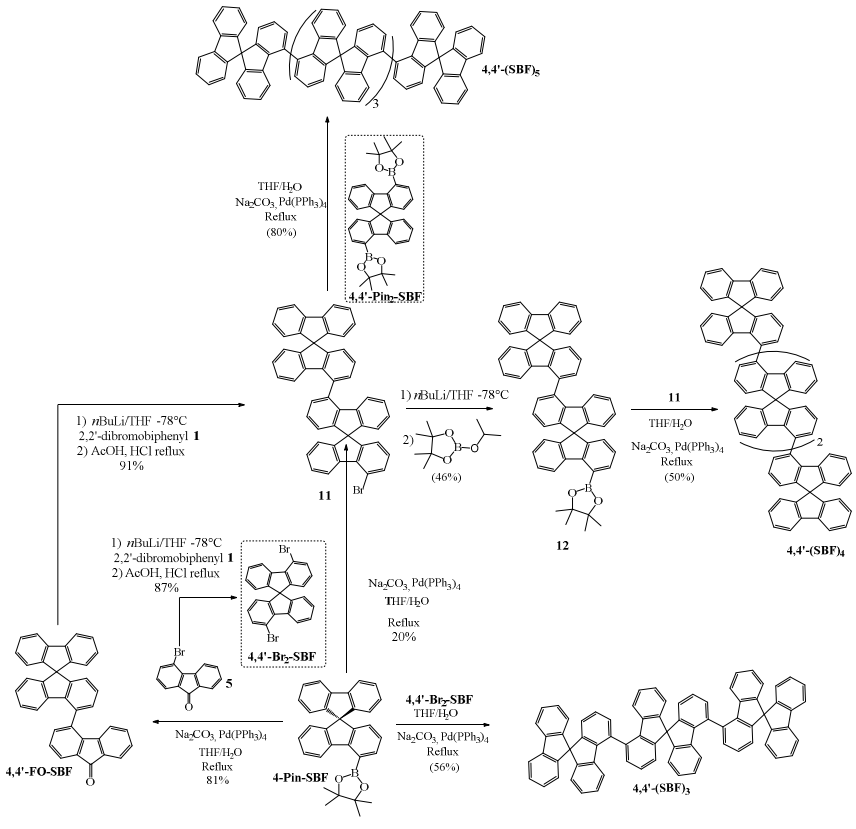

Figure 10. Synthesis of the SBF oligomers **4,4'-(SBF)$_3$**, **4,4'-(SBF)$_4$** and **4,4'-(SBF)$_5$**

Finally, **DSF[2,1-*c*]IF** can be seen as a **4-Ph-SBF** fragment, whith the pendant phenyl ortho-bridged to the SBF unit in C3 by a second spirofluorene core. It has been synthesised in a multistep route starting from the coupling of **4-Br-SBF** with 2-(ethoxycarbonyl)phenylboronic acid providing after intramolecular ring closure the spirofluorene-indeno[2,1-*c*]fluorenone **10**. **DSF[2,1-*c*]IF** was then classically obtained by coupling the ketone **10** with 2-bromobiphenyl **4**, followed by the intramolecular ring closure (24% yield over the three last steps).[3]

Access to longer oligospirobifluorenes, **4,4'-(SBF)$_3$**, **4,4'-(SBF)$_4$** and **4,4'-(SBF)$_5$** first involved the synthesis of **4,4'-Br$_2$-SBF** and its related pinacol **4,4'-Pin$_2$-SBF** (figure 10). **4,4'-Br$_2$-SBF** was synthesised by reaction of **5** with 1 equivalent of (2-bromobiphenyl-2-yl)lithium followed by an intramolecular cyclisation (87 % yield). **4,4'-Br$_2$-SBF** was then converted to its pinacol **4,4'-Pin$_2$-SBF** in classical conditions. The coupling of **4,4'-Br$_2$-SBF** with two equivalents of **4-Pin-SBF** then leads to the SBF trimer **4,4'-(SBF)$_3$** in good yields (56 %). The same coupling of **4,4'-Br$_2$-SBF** with only one equivalent of **4-Pin-SBF** leads to the brominated-SBF dimer **11** in a rather low yield (20%) due to the simultaneous formation of **4,4'-(SBF)$_3$**. Another route to **11** is also reported in two steps: (i) coupling of **4-Pin-SBF** with **5** leading to the 4-(4-fluorenone)-spirobifluorene **4,4'-FO-SBF** and (ii) reaction of **4,4'-FO-SBF** with **1** followed by an intramolecular ring-closure. This two steps route provides **11** with a yield of 74% (from **4-Br-SBF**) being higher than the previously mentioned approach. Thus, the tetramer **4,4'-(SBF)$_4$** can be synthesized by the coupling of the dimer **11** with its pinacol **12** (yield =50 %). Finally, the pentamer **4,4'-(SBF)$_5$** was afforded by treated one equivalents of **11** with one equivalent of **4,4'-Pin$_2$-SBF** through Suzuki coupling (80 % yield).

Structural Properties

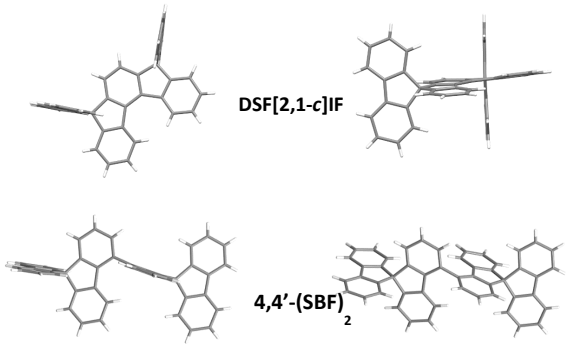

Figure 11. X-ray structures of **DSF[2,1-*c*]IF** (top)[3] and **4,4'-(SBF)$_2$** (bottom).[70]

We have stressed above the importance of the dihedral angle between the pendant substituent and the fluorene. In the case of **4,4'-(SBF)$_2$**, an angle as high as 88.3° is reported (figure 11-bottom)[70] being impressively larger than that of **4-Ph-SBF** (*ca* 50°).[81] This angle has important consequences on the electronic properties which are described below. Unfortunately, as far as we know, no other X-ray data are reported for other PHC based on the 4-substituted SBF core with pendant groups. Dispiro[fluorene-9,5'-indeno[2,1-c]fluorene-8',9''-fluorene] (**DSF[2,1-*c*]IF**) appears as a particular example as there is no pendant group in C4 but instead a bridged spirofluorene (C4 and C3 substitution). **DSF[2,1-*c*]IF** is hence a bridged analogue of **4-Ph-SBF**. Thus, in **DSF[2,1-*c*]IF**, the substituent in C4 is almost planar with a dihedral angle of 13° between the two side phenyl rings of the dihydroindenofluorene core (figure 11-top).[3] Due to this bridge rigidification and the resulting planar structure, the electronic properties appear to be different to those described for the other 4-substituted SBFs (see below). This clearly shows the chief role played by the dihedral angle in such compounds.

Electronic properties

In order to describe the general behaviour of 4-substituted SBFs in absorption spectroscopy, the couple **SBF/4-Ph-SBF** has been choosen as a representative example. **DSF[2,1-*c*]IF**[3] with its fused structure will be also used herein for comparison purpose. The UV-Vis absorption spectrum of **4-Ph-SBF** (in cyclohexane) exhibits at low energy two thin absorption bands at 296 and 308 nm, similar to those observed for **SBF** (figure 12, left)[81, 91] and for the other 4-substituted oligo-SBFs such as **4,4'-(SBF)$_2$**, **4,4'-(SBF)$_3$**, **4,4'-(SBF)$_4$** or **4,4'-(SBF)$_5$**.[69, 70] However, for **4-Ph-SBF**, the band at 308 nm clearly presents a longer wavelength tail leading to an optical energy gap (ΔE^{opt}) of 3.82 eV, more contracted by 0.15 eV than that of **SBF** (3.97 eV). The absorption tail of **4-Ph-SBF** is the consequence of the substitution in position 4. Indeed, although the π-conjugation of **4-Ph-SBF** is strongly disrupted compared to that of its *para*-linked regioisomer **2-Ph-SBF** (λ_{max}=319 nm, ΔE^{opt}=3.70 eV),[82] this tail reflects nevertheless a certain degree of π-conjugation between the phenyl ring and the fluorene moiety. Thus, in **4-Ph-SBF**, the π-conjugation is not completely broken but strongly disrupted. The gap contraction observed for **4-Ph-SBF** is nevertheless more pronounced than that of highly twisted oligo-SBFs **4,4'-(SBF)$_2$**, **4,4'-(SBF)$_3$**, **4,4'-(SBF)$_4$** or **4,4'-(SBF)$_5$** which possess a ΔE^{opt} of 3.93 eV, independent of the number of SBF units,[69, 70] being hence almost identical to that of **SBF** (3.97 eV). This feature finds its origin in the very large fluorene/fluorene dihedral angle of 88.3° reported for **4,4'-(SBF)$_2$** (Figure 11, bottom), which leads to an almost complete π-conjugation interruption.[70] Thus, the bulkiness induced by the presence of the substituent in C4 and hence the angle formed between this substituent and the fluorenyl unit has a marked effect on the π-conjugation intensity. **DSF[2,1-*c*]IF** confirms the key importance of this angle on the electronic properties of 4-substituted SBFs. Indeed, the absorption maximum of **DSF[2,1-*c*]IF** is reporded at 338 nm, being strongly red shifted compared to those of **4-Ph-SBF** and **4,4'-(SBF)$_2$**. Indeed, due to the bridge rigidification, a very small angle of only 13° is reported for this molecule (Figure 11, top), and the π-conjugation is hence maximised. This feature clearly shows that the π-conjugation disruption observed in 4-substituted SBFs finds its origin in the large dihedral angle formed between the fluorene and the substituent and not in the electronic decoupling.[4]

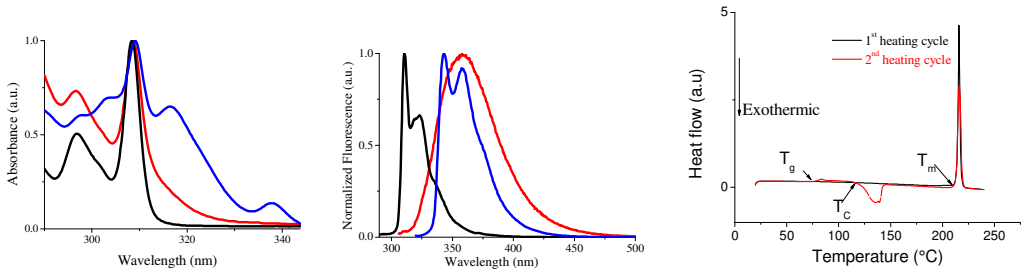

Figure 12. Absorption (left) and Emission (middle) spectra of **4-Ph-SBF** (red line), **DSF[2,1-*c*]IF** (blue line) and **SBF** (back line) in cyclohexane, C=10^{-6} M, DSC curves of **4-Ph-SBF** (right).

Despite very similar properties in the fundamental state, **4-Ph-SBF** and **SBF** display remarkable but surprising differences in their excited states (figure 12, middle).[81] Indeed, **4-Ph-SBF** exhibits a structureless emission spectrum (λ_{max}=358 nm), noticeably different in shape and wavelength compared to that of **SBF**,[81, 91] which presents a well-resolved spectrum (λ_{max}=310/323 nm) mirror image of its absorption spectrum. This large and unresolved band is found for all the dyes exclusively built on the 4-substituted SBF scaffold such as **4,4'-(SBF)$_2$** (λ_{max}=373 nm), **4,4'-(SBF)$_3$**, **4,4'-(SBF)$_4$**, **4,4'-(SBF)$_5$** (λ_{max}=374 nm),[69] and **4,3'-(SBF)$_2$** (λ_{max}=370 nm).[88] This band is also found for other SBF compounds possessing a combination of *para* and *ortho* linkages such as **2,7,4'-(SBF)$_3$**.[70] This surprising loss of resolution of the emission spectrum is also observed for the other examples of 4-substituted SBFs described in the following of this review (except **4-PhCbz-SBF** (4-N-phenyl-carbazole-9,9'-spirobi[fluorene]), which is a particular example precisely described in part 6). Indeed, this feature appears hence to be a unique characteristic of 4-substituted-SBF derivatives as 2-substituted-SBF analogues always present well resolved emission bands assigned to the double bond character of the C-C bond linking the pendant substituent and the fluorenyl core in the excited state.[8, 9, 83, 92, 93] Thus, **2,2'-(SBF)$_3$** and **2,2'-(SBF)$_2$** exclusively built on para linkages present a well resolved emission spectrum,

drastically different to those of their 4-substituted analogues, namely **4,4'-(SBF)$_2$** and **4,4'-(SBF)$_3$**. The same conclusion can be drawn for **2-Ph-SBF** and **4-Ph-SBF**.[82] If it seems clear nowadays that the position of the substitution (C2 *vs* C4) is at the origin of this spectacular effect, no complete answer has been provided in the literature yet.[71, 81, 82, 94] However, some recent findings on **4-PhCbz-SBF** (see structure in Figure 23) seem to shed light on this peculiar behaviour, which will be discussed in part 6.[95] **DSF[2,1-*c*]IF** highlights the importance of the planarization on the emission properties.[3] Indeed, and oppositely to the other 4-substituted-SBFs above described, **DSF[2,1-*c*]IF** presents a well-resolved emission spectrum with two thin bands at 343 and 358 nm (Figure 12, middle), confirming the cancelation of 'the 4-substituent effect'. This is due to the rigid and almost flat dihydroindeno[2,1-*c*]fluorene core, which only allows very weak molecular motions.

It is always difficult to accurately compare the quantum yields of different molecules as the experimental conditions (solvent, reference etc) need to be identical. The quantum yield (Φ_{sol}) of **4-Ph-SBF** is reported at 0.4 being identical to that of **SBF** and more than twice inferior to that of its regioisomer **2-Ph-SBF**, 0.87.[71] The higher quantum yield of **2-Ph-SBF** vs **4-Ph-SBF** is explained by the authors by a combination of higher radiative rate constant k_r (k_r of 5.6×10^8 and 1.0×10^8 s^{-1} *resp.*) and smaller non radiative rate constant k_{nr} (8.3×10^7 and 1.4×10^8 s^{-1} *resp.*). The SBF oligomers **4,4'-(SBF)$_3$**, **4,4'-(SBF)$_4$** and **4,4'-(SBF)$_5$** all present similar Φ_{sol} of 0.63, 0.58 and 0.6 respectively.

To insure efficient host-guest energy transfers in the Emitting layer (EML) of a PhOLED[96, 97] and to avoid back energy transfers from the guest to the host, the E_T of the host should be higher than that of the guest. The determination of the E_T of an organic host is hence an important feature in this research field. As organic materials are very often not emissive from their excited triplet state T_1 at room temperature, the E_T is usually evaluated by the first phosphorescent peak of the emission spectrum recorded at 77 K. We have seen above, the strong impact of the SBF substitution in position 4 on the absorption and emission spectra at room temperature but what are the repercussions at 77K and hence on the E_T?

First, the E_T of **SBF** has been reported at 2.87 eV being slightly lower than that of its building block fluorene (E_T=2.92 eV).[81] The slight conjugation between the two fluorene units in **SBF** (called spiroconjugation)[91, 98-102] decreases the E_T of **SBF** by *ca* 0.05 eV compare to fluorene.[81, 91] All the PHC derivatives exclusively built on *ortho* linkages possess a similar E_T, measured at 2.77 eV for **4-Ph-SBF** and close to 2.80 eV for the oligo-SBFs, **4,4'-(SBF)$_2$**, **4,4'-(SBF)$_3$**, **4,4'-(SBF)$_4$** or **4,4'-(SBF)$_5$**. As the building unit **SBF** presents an E_T of 2.87 eV, a decrease of ca 0.05/0.1 eV is reported for the molecules above mentioned. This highlights that (i) the π-conjugation is not completely broken and that (i) the nature and the number of substituents do not strongly impact the E_T. For comparison, **2,2'-(SBF)$_3$** and **2,7,2'-(SBF)$_3$**, both built on *para* linkages possess a E_T of 2.28 eV,[89] impressively smaller than those of the *ortho* linked SBFs above described. Indeed, due to the *para* linkages of 2-substituted SBFs, there is an electronic delocalization on the two connected fluorenes and the E_T is hence very low. Thus, the steric congestion induced by the *ortho* linkage of 4-substituted SBFs leads to significant E_T increase of ca 0.5 eV compared to the 2-substituted analogues. This feature highlights the strong impact of the substitution position (2 vs 4) to increase the E_T. **2,7,4'-(SBF)$_3$** nicely illustrates this position effect. Indeed, this SBF trimer possesses an intermediate E_T of 2.55 eV, being smaller than the fully *ortho* linked SBF trimer **4,4'-(SBF)$_3$** but higher than the fully *para* linked one **2,2'-(SBF)$_3$**. This is the consequence of the combination (i) of the *para* linkages of the 2,7-substituted SBF, which decreases the E_T due to the extension of the conjugation and (ii) of the *ortho* linkages which leads to a sterically hindered environment. Similar observations can be made for the SBF dimers, which E_T decreases from 2.81 to 2.76 and 2.3 eV for **4,4'-(SBF)$_2$** to **4,3'-(SBF)$_2$** and **2,2'-(SBF)$_2$**. Interestingy, **4,3'-(SBF)$_2$** described by Liao et al.[88] is a SBF dimer possessing a different position of substitution on each SBF: a *meta* and an *ortho* linkage. The partial electronic decoupling induced by the *meta* substitution coupled to the steric hindrance induced by the *ortho* substitution leads to a high E_T of 2.76 eV. Finally, **DSF[2,1-*c*]IF**, due to its extended central backbone, possesses an E_T of 2.63 eV[3] being lower than those described above for the 4-substituted oligo-SBFs. Indeed, in **DSF[2,1-*c*]IF**, due to the ring bridging, the dihedral angle is small (13°) maximising hence the conjugation and in turn decreasing the E_T.

Thermal properties

The thermal properties of an OSC are key features before any integration into an electronic device. Indeed, it is known that the temperature of an OLED increases upon working due to Joule effect and can reach temperature as high as 90°C.[103] The stability of the constituted materials is hence of great importance to notably avoid the decomposition of the material during the device working. Two parameters play a key role: the decomposition temperature (T_d) obtained by Thermogravimetric Analysis (TGA) and the glass transition temperature (T_g) obtained by Differential Scanning Calorimetry (DSC). The T_d is defined as the temperature at which the sample has lost the first 5% of its mass.[2, 104] This temperature can also be seen in some cases as the sublimation temperature. Indeed, the sublimation of the material at high temperature may also lead to a total mass loss. Spiro compounds usually possess very high T_d due to their bulky shape.[2, 104] **4-Ph-SBF** presents a T_d of 254°C, slightly higher than that of its regioisomer **2-Ph-SBF** and that of its building block **SBF** (238 and 234°C *resp.*). Switching from phenyl to SBF leads to a strong enhancement of the T_d reporded at 360°C for **4,4'-(SBF)$_2$**, and at 367°C for its regioisomer **2,2'-(SBF)$_2$**. Increasing the size of the molecule by connecting more SBF units also leads to a considerable increase of the T_d (464°C for **2,2'-(SBF)$_3$** and 535°C for **2,7,4'-(SBF)$_3$**). **DSF[2,1-*c*]IF** also presents a high T_d of 347°C, highlighting the strong impact of the bridge rigidification on the T_d.

Generally spiro compounds are also characterized by a high T_g, this is even one of their most appealing property.[2, 104, 105] A characteristic example of DSC curve is presented for **4-Ph-SBF** (Figure 12, right). **4-Ph-SBF** presents on the first heating, a sharp endothermic peak at 216°C associated to its melting. When the isotropic liquid was cooled down, no recristallization occurs and the cooling leads then to an amorphous solid. When the amorphous glass was heated again, a T_g was detected at 76°C (from peak onset). On further heating above the T_g, an exothermic peak caused by crystallization was observed at 139°C followed by the sharp endothermic fusion peak at 216°C. This thermal behaviour is typical of organic glasses.[2, 106] Thus, **4-Ph-SBF** possesses a T_g almost identical to that of its isomer **2-Ph-SBF** (T_g=78°C). Switching from phenyl in **4-Ph-SBF**/**2-Ph-SBF** to SBF in **4,4'-(SBF)$_2$**/**2,2'-(SBF)$_2$**, leads to a significant T_g increase respectively reported at 170 and 174°C. Thus, the substituent borne by the SBF has a strong impact on its T_g but the position of substitution (4 *vs* 2) not. This is also highlighted for the other SBF dimers. Indeed, **4,4'-(SBF)$_2$**, **4,3'-(SBF)$_2$**, **2,2'-(SBF)$_2$** all possess a T_g at 170°C/180°C being hence weakly dependent on the substitution. However, the incorporation of extra SBF fragments in **4,4'-(SBF)$_3$**, **4,4'-(SBF)$_4$** and **4,4'-(SBF)$_5$** has a significant impact as it leads to a further T_g increase, reported at 244, 280 and 326°C *resp.*. Thus, as the number of SBF units increases, the T_g increases as well. Thus, we have shown above that the electronic properties and notably the E_T is identical for the four oligomers (ca 2.8 eV), whereas the T_g is strongly increased by 156°C from **4,4'-(SBF)$_2$** to **4,4'-(SBF)$_5$**. This is one of the key advantages of the spiro bridge: keeping an electronic property and enhancing the physical properties.

Table 1. Selected electronic and physical data for PHC compounds presented in part 4

	λ_{abs} (nm)	λ_{fluo} (nm)	E_T (eV)	Φ_{sol}	HOMO[a]	LUMO	ΔE_{opt}[e]	T_g	T_d
4-Ph-SBF [81]	308 (+ sh)	358	2.77	0.4	−5.95[a]	−1.95[a]	3.82	76	254
2-Ph-SBF [71]	319	335, 351	2.56	0.84	−5.88[a]	−2.10[a]	3.70	78	238
SBF [81]	308	310, 323	2.87	0.40	−5.94 [a]	−1.89[a]	3.97	no	234
4,4'-(SBF)$_2$ [70]	309	373	2.81	-	-	-	-	170	360
4,4'-(SBF)$_3$ [69]	308	374	2.80	0.63	-6.08 [a]	-2.15 [c]	3.93	244	-
4,4'-(SBF)$_4$ [69]	308	374	2.80	0.58	-6.08[a]	-2.15 [c]	3.93	280	-
4,4'-(SBF)$_5$ [69]	308	374	2.80	0.60	-6.08[a]	-2.15 [c]	3.93	326	-
4,3'-(SBF)$_2$ [88]	318	370	2.76	-	-5.76[b]	-2.11 [c]	3.65	177	407
DSF[2,1-*c*]IF[3]	338	343, 358	2.63	0.5	-5.87	-2.00	3.60	no	347
2,7,4'-(SBF)$_3$ [70]	309/325	390	2.55	-	-	-	-	232	535
2,2'-(SBF)$_2$ [89]	333	367/387	2.30	0.66[d]	-	-	-	174	367
2,2'-(SBF)$_3$ [89]	333	367/387	2.28	0.56[d]	-	-	-	228	464

2,7,2'-(SBF)$_3$ [90]	350	-	-	-	-	-	-	237	-
2,7,2'-(SBF)$_4$ [90]	360	-	-	-	-	-	-	258	-

[a.] From CV, [b.] from UPS, [c.] from ΔE^{opt} and HOMO, [d.] as thin film with an integrated sphere, [e.] from the absorption spectrum λ_{onset}, -: not reported in literature, no: not observed

Phosphorescent OLEDs

Performances of red, green or blue PhOLEDs using the 4-substituted SBFs as hosts are presented below. The red emitting Iridium complexes used below are bis(2,4-diphenylquinolyl-N,C2')iridium(acetylacetonate) ((ppq)$_2$Ir(acac)) (E_T: 2.01 eV) or bis[2-(20-benzo[4,5-a]thienyl)pyridinato-N,C30] iridium(acetylacetonate) ((Btp)$_2$Ir(acac)) (E_T: 2 eV),[89] the green emitting one is tris[2-phenylpyridinato-C^2,*N*]iridium(III) (Ir(ppy)$_3$) (E_T: 2.42 eV), and the sky blue emitting one is bis[2-(4,6-difluorophenyl)pyridinato-C^2,*N*](picolinato)iridium(III) (FIrpic) (E_T: 2.62 eV).[107]

Table 2. Selected EL data of red, green and blue devices using PHC compounds presented in part 4

Host E_T	**Dopant** doping level	V_{on} (V)	E.Q.E (%)	CE (cd/A)	PE (lm/W)	Ref
			Red Devices			
2,2'-(SBF)$_3$ [a] 2.28 eV	Btp$_2$Ir(acac) 8 wt %	2.5/3.0	8.6 @0.3 mA/cm^2	-	4 (max value)	89
2,7,4'-(SBF)$_3$ [b] 2.55 eV	(ppq)$_2$Ir(acac) 6 wt %	5.5	10.5 (max value)	8.4 (max value)	4.1 (max value)	70
			Green Devices			
2,7,4'-(SBF)$_3$ [b] 2.55 eV	Ir(ppy)$_3$ 8 wt %	4	12.6 (max value)	48.2 (max value)	26.8 (max value)	70
4,4'-(SBF)$_3$ [c] 2.80 eV	Ir(ppy)$_3$ 11 wt %	-	17.3 (max value)	66 (max value)	46 (max value)	69
SBF [d] 2.87 eV	Ir(ppy)$_3$ 9 wt %	3.1 @ 1 cd/m^2	8.5 (max value)	33.4 (max value)	20.5 (max value)	81
4-Ph-SBF [d] 2.77 eV	Ir(ppy)$_3$ 9 wt %	3.5 @ 1 cd/m^2	10.4 (max value)	48.1 (max value)	36 (max value)	81
DSF[2,1-*c*]IF [d] 2.63 eV	Ir(ppy)$_3$ 10 wt %	3.0 @ 1 cd/m^2	13.3 (max value)	49.0 (max value)	26.6 (max value)	3
			Sky-blue Devices			
4,4'-(SBF)$_3$ [c] 2.80 eV	FIrpic 8 wt %	-	11.6 (max value)	25 (max value)	17 (max value)	69
4,3'-(SBF)$_2$ 2.76 eV	FIrpic 8 wt %	3.0	22 (max value)	44.5 (max value)	36.5 (max value)	88
SBF [d] 2.87 eV	FIrpic 19 wt %	3.3 @ 1 cd/m^2	6.6 (max value)	20.6 (max value)	-	81
4-Ph-SBF [d] 2.77 eV	FIrpic 19 wt %	4.0 @ 1 cd/m^2	5.7 (max value)	18.4 (max value)	-	81

- : not reportedDevice structure [a] :ITO/PEDOT-PSS(30 nm)/TCTA(30 nm)/Host-Guest(30 nm)/BCP(10 nm)/Alq$_3$(60 nm)/LiF(0.5 nm)/Al,
[b] : ITO/MoO$_3$(10 nm)/NPB(40 nm)/ Host-Guest(30 nm)/BCP(10 nm)/Alq$_3$(30 nm)/LiF(1 nm)/Al(100 nm)
[c]: ITO/MoO$_3$(10 nm)/NPB(80 nm)/TCTA(5 nm)/ Host-Guest(20 nm)/TPBi(30 nm)/LiF(1 nm)/Al(120 nm)
[d]: ITO/CuPc(10 nm)/NPB(40 nm)/TCTA(10 nm)/ Host-Guest (20 nm)/TPBi(40 nm)/LiF(1.2 nm)/Al(100 nm)

The first example has been reported with the trimer **2,2'-(SBF)$_3$**.[89] Due to its low E_T of 2.28 eV, this molecule has been only incorporated in a red device with the following architecture ITO/PEDOT-PSS(30nm)/TCTA(30nm)/**2,2'-(SBF)$_3$**:(Btp)$_2$Ir(acac)(30nm)/BCP(10nm)/Alq$_3$(60nm)/LiF(0.5nm)/Al. This device, with the red phosphor (Btp)$_2$Ir(acac) in 8 wt%, presents a maximal External Quantum Efficiency (EQE) of 8.6% and a maximal Power Efficiency (PE) of 4 lm/W. As above mentioned, switching from *para* linkages in **2,2'-(SBF)$_3$** to *para* and *ortho* linkages in **2,7,4'-(SBF)$_3$** allows to strongly increase the E_T (from 2.28 to 2.55 eV, Table 1). Thus, **2,7,4'-(SBF)$_3$** was used as host not only in red emitting devices

(dopant $(ppq)_2Ir(acac)$) but also in green emitting ones (dopant $Ir(ppy)_3$) with the following architecture ITO/MoO_3(10nm)/NPB(40nm)/**2,7,4'-(SBF)$_3$**:dopant(30nm)/BCP(10 nm)/Alq_3(30 nm)/LiF(1 nm)/Al(100 nm).[70] With the green dopant $Ir(ppy)_3$ 8 wt%, the device displays a Current Efficiency (CE) of 48.2 cd/A, a maximum PE of 26.8 lm/W and an EQE of 12.6%. The performance is lower with the red dopant $(ppq)_2Ir(acac)$ in 6 wt%, with a CE of 8.4 cd/A, a PE of 4.1 lm/W and a maximum EQE of 10.5%.

The trimer **4,4'-(SBF)$_3$** has been incorporated in both green and blue PhOLEDs.[69] The structure was ITO/MoO_3(10nm)/NPB(80nm)/TCTA(5nm)/**4,4'-(SBF)$_3$**:dopant(20nm)/TPBi(30nm)/LiF(1nm)/Al(120nm). The green device ($Ir(ppy)_3$ 11 wt%) displays a max EQE of 17.3%, a CE of 66 cd/A and a PE of 46 lm/W and the sky blue device (FIrpic 8 wt %) displays a max EQE of 11.6%, a CE of 25 cd/A and a PE of 17 lm/W.
In this research field, it is always difficult to accuretaly compare the efficiency of a host within a device. Indeed, the device structure (and not only the host) has a strong importance in the performance. Thus and in order to accurately compare the performance of the hosts, the device architecture should be strictly identical. In the literature, the device performances are presented in many different ways (maximum values or at 1 or 10 mA/cm^2 principally) rendering their comparison very difficult.

Interestingly, as **4-Ph-SBF**, **SBF** and **DSF[2,1-*c*]IF** have been incorporated as host in PhOLEDs possessing an identical architecture, the different device performances can be hence only imputed to the host. The device configuration was: ITO/CuPc(10 nm)/NPB(40 nm)/TCTA(10 nm)/Host:$Ir(ppy)_3$(20 nm) or Host: FIrpic(20 nm)/TPBi(40 nm)/LiF(1.2 nm)/Al(100 nm) for green or blue devices respectively. The green device with **4-Ph-SBF**:$Ir(ppy)_3$ in 9 wt% as EML has a low threshold voltage V_{on} of 3.5 V, with maximum CE and PE of 48.1 cd/A and 36 lm/W *resp.*, equivalent to an EQE of 10.4%.[81] **SBF** in identical conditions presents lower performance (CE=33.4 cd/A, PE= 20.5 lm/W and EQE= 8.5%) with nevertheless a slightly lower V_{on} of 3.1 V.[81] Thus, the incorporation in C4 of a phenyl ring in **4-Ph-SBF** allows increasing the EQE of green devices, highlighting the efficiency of this design. Device with **DSF[2,1-*c*]IF**:$Ir(ppy)_3$ in 10 wt% as EML presents the highest performance in the series with CE= 49.0 cd/A, PE= 26.6 lm/W, EQE = 13.3% and V_{on}=3 V.[3] Thus, the performance follows the trend: **DSF[2,1-*c*]IF**>**4-Ph-SBF**>**SBF**, indicating that the C4-substitution and the bridge rigidification both have a key role in the PhOLED performance.

Blue PhOLEDs appear to follow a different trend, highlighting the difficulty to design universal hosts. Indeed, with **SBF** as host (FIrpic: 19 wt%), the device presents a CE of 20.6 cd/A, an EQE of 6.6% with a V_{on} of 3.3 V whereas with **4-Ph-SBF** as host (FIrpic 19 wt%), the device efficiency is slightly lower (EQE= 5.7 % and CE= 18.4 cd/A).[81] Due to its E_T of 2.63 eV, almost identical to that of FIrpic, **DSF[2,1-*c*]IF** has not been incorporated in a blue device.[3]

Finally, the best performance for such PHC derivatives has been reported by Liao, Jiang and their co-workers with the *ortho/meta* dimer **4,3'-(SBF)$_2$**.[88] The device configuration was : ITO/HAT-CN(10nm)/ TAPC(40nm)/**4,3'-(SBF)$_2$**:FIrpic(8wt%)(20nm)/TmPyPB(45nm)/Liq(2nm)/Al(120nm). With such device, the authors report a very high maximum EQE of 22% with corresponding CE of 44.5 cd/A and PE of 36.5 lm/W and a V_{on} of 3.0 V. The authors explain this high performance by a combination of two main parameters. First, the MLCT absorption of FIrpic is largely overlapped with the emission of **4,3'-(SBF)$_2$** implying effective energy transfers from **4,3'-(SBF)$_2$** to FIrpic and second, the ambipolar character of **4,3'-(SBF)$_2$**, which is a key feature for charge transport.

5. 4-Substituted SBF incorporating electron accepting units.

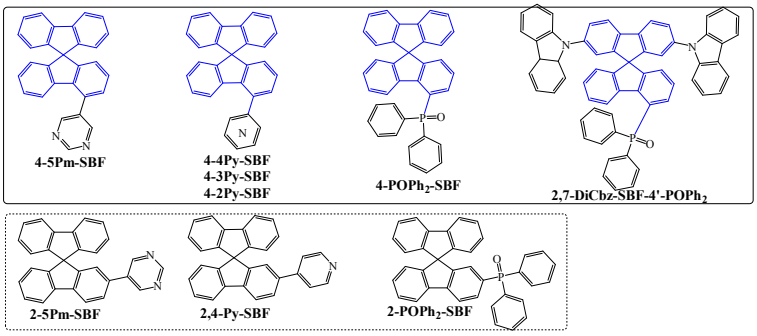

Figure 13: 4-(Top) and 2-(bottom) substituted SBFs incorporating electron-withdrawing fragments

Numbers of electron withdrawing functionalities have been introduced on the SBF scaffold in order to make the electronic properties of the resulting dyes fitting with a specific application.[2] For that purpose, electron-deficient heterocycles such as 1,3,4-oxadiazoles,[108,66, 109] pyridine,[110] quinoline,[111] quinoxaline,[112] pyrimidine,[113, 114] and pyridopyrazine[115] have been introduced on the SBF core but most of the time in 2, 2' and/or 7, 7' positions. As 4-substituted SBFs remain weakly studied to date, only few examples incorporating electron-accepting fragments have been reported as host in PhOLEDs.

Diphenyl-9,9'-spirobi[9*H*-fluoren]-4-yl-phosphine oxide (**4-POPh$_2$-SBF**) first reported by Lee and co-workers in 2010 is built on a SBF backbone possessing in position 4 a phosphine oxide group.[116] Our group has reported in 2015 a structurally related compound, namely **2,7-DiCbz-SBF-4'-POPh$_2$** (9,9'-(4'-diphenyl-phosphine oxide-9,9'-spirobi[9*H*-fluorene]-2,7-diyl)bis-9*H*-carbazole).[53] This molecule is similar to **4-POPh$_2$-SBF** as it possesses a 4-phosphine oxide-fluorene but the spirolinked fluorene is flanked with two N-carbazoles units in positions 2' and 7'. The four other examples incorporate in C4 either a 5-pyrimidine ring (**4-5Pm-SBF**)[82] or pyridine isomers (**4-4Py-SBF**, **4-3Py-SBF** and **4-2Py-SBF**).[71] In a structure properties relationship approach, 2-substituted analogues incorporating either a 4-pyridine (**2-4Py-SBF)**, a 5-pyrimidine (**2-5Pm-SBF**) or a phosphine oxide (**2-POPh$_2$-SBF)** have been also reported herein in order to shed light on the impact of the substituents position on the SBF scaffold.

Synthesis

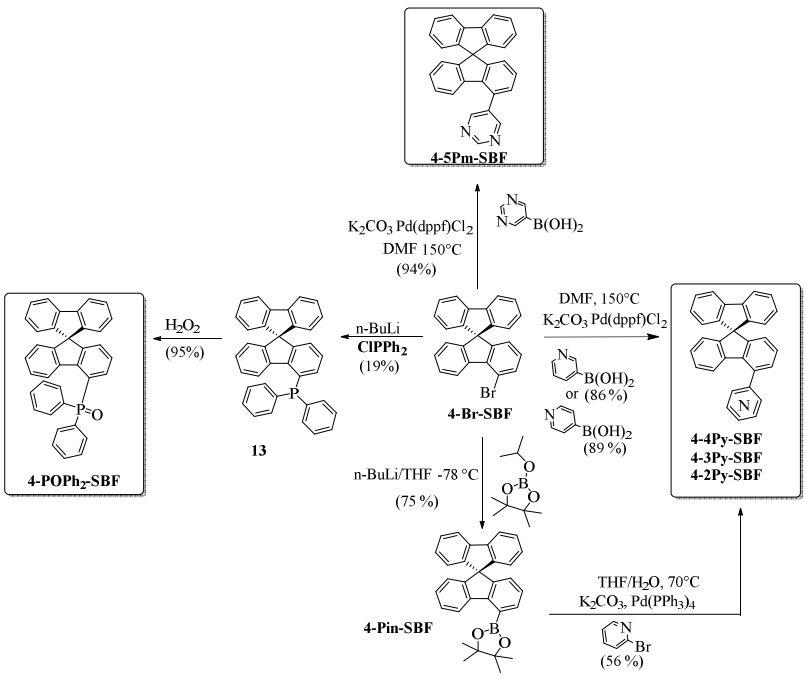

Figure 14. Synthesis of **4-4Py-SBF**,[71] **4-3Py-SBF**,[71] **4-2Py-SBF**,[71] **4-5PmSBF**[82] and **4-POPh$_2$SBF**[116]

The synthesis of these 4-substituted SBFs implies, as above mentioned, the key building block **4-Br-SBF**. Thus, as presented figure 14, Suzuki cross-couplings ($Pd(dppf)Cl_2/K_2CO_3$/ DMF) between **4-Br-SBF** and either 4- or 3-pyridine-phenyl boronic acid provide **4-4Py-SBF** and **4-3Py-SBF** with excellent yields of 89 and 86% *resp*.[71] However, the instability of 2-pyridine-phenyl boronic acid does not allow its coupling with **4-Br-SBF** and the synthesis of **4-2Py-SBF** has been performed via a modified approach involving the cross-coupling of **4-Pin-SBF** and 2-bromopyridine (overall yield 42% from **4-Br-SBF**).[71] Similarly, Suzuki cross-coupling between **4-Br-SBF** and 5-pyrimidine boronic acid provides **4-5Pm-SBF** with 94% yield. [82] The model compounds **2-4Py-SBF**[71] and **2-5Pm-SBF**[82] (figure 13, bottom) were obtained through similar pathways from the 2-bromo-9,9'-spirobifluorene (yield : 82% and 77% *resp.*).
4-$POPh_2$-SBF was synthetized through the treatment of **4-Br-SBF** with n-BuLi, followed by the trapping of the resulting lithiated intermediate with chlorodiphenylphosphine ($ClPPh_2$) (yield 19%).[116] The corresponding 4-diphenylphosphine-SBF **13** obtained was further oxidized (H_2O_2) to provide **4-$POPh_2$-SBF** with 95% yield. The 2-substituted isomer **2-$POPh_2$-SBF** was synthetized using an identical approach.[110]

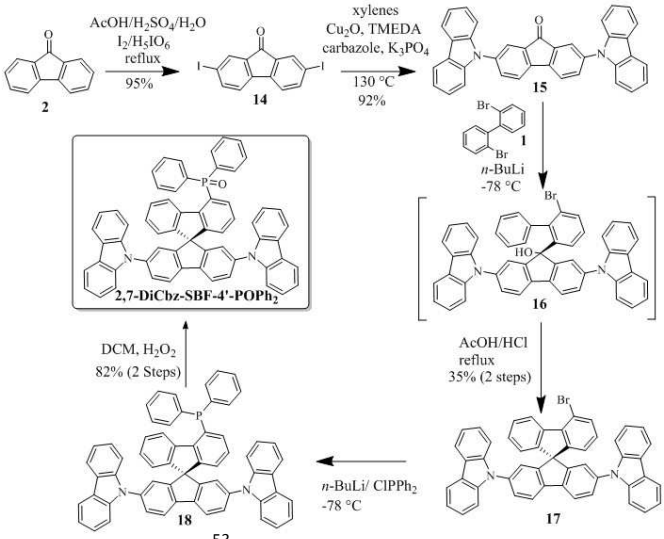

Figure 15. Synthesis of **2,7-DiCbz-SBF-4'-$POPh_2$**[53]

As the molecular structure of **2,7-DiCbz-SBF-4'-$POPh_2$** is more elaborated, it has been synthesized following a different route involving the coupling of the 2,7-dicarbazole-fluorenone **15** with 2,2'-bromobiphenyl **1** (Figure 15).[53] The resulting fluorenol **16** is then involved in an intramolecular ring closure to provide **17** (35% yield, 2 steps). Incorporation of the phosphine oxide was then classically performed through the following sequence: (i) lithium-halogen exchange on **17** (ii) trapping of the lithiated intermediate with **$ClPPh_2$** to provide the diphenylphosphine derivative **18** and (iii) oxidation of the phosphorus atom with H_2O_2 to give the target **2,7-DiCbz-SBF-4'-$POPh_2$** (yield=82% over the two last steps). The overall yield of this approach is rather high (25%) and does not use any Pd catalyst.

Structural properties

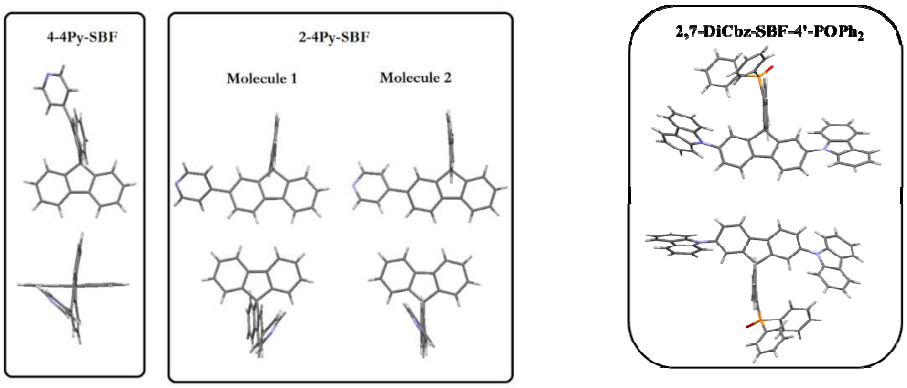

Figure 16. X-ray structures of **4-4Py-SBF** (left),[71] **2-4Py-SBF** (middle)[71] and **2,7-DiCbz-SBF-4'-POPh$_2$** (right)[53]

As mentioned in part 3, the π-conjugation breaking observed in 4-substituted SBFs is induced by the large dihedral angle between the fluorene and the pendant substituent. Figure 16 reports the X-ray structures of **4-4Py-SBF**,[71] **2-4Py-SBF**[71] and **2,7-DiCbz-SBF-4'-POPh$_2$**.[53] In **4-4Py-SBF**, the pyridyl/fluorene dihedral angle is reported at 42.2°, being slightly higher than that of its C2 isomer **2-4Py-SBF** (37.5° and 32.8° as two molecules are present in the asymmetric unit). The angular difference between the 2 isomers (less than 9.4°) is hence smaller than that reported above between **2-Ph-SBF** and **4-Ph-SBF** (around 13.8°)[81] translating the influence of the substituent (pyridine *vs* phenyl) on this chief structural parameter which controls the electronic properties. Indeed, we will see below that this angular variation leads to a more extended π-conjugation between the pyridine and the fluorene in **4-4Py-SBF** than between the phenyl and the fluorene in **4-Ph-SBF**. An intense deformation of the substituted fluorene core (16.8°) is also observed in **4-4Py-SBF** which is more pronounced than that reported for **4-Ph-SBF** (12.7°)[81] and for **2-4Py-SBF** (3.2° and 5.0° for the two molecules).[71] The comparison of these 2 couples **4-4Py-SBF/2-4Py-SBF** and **4-Ph-SBF/2Ph-SBF** indicates that the fragment attached in C4 has a strong influence on the structural parameters and hence on the π-conjugation intensity with the fluorene.

Oppositely to the other 4-substituted SBFs described above, in which the conjugation is only broken by a steric congestion, the conjugation between the phosphine oxide and the fluorene is also broken by the phosphorus atom in **2,7-DiCbz-SBF-4'-POPh$_2$**.

Electronic properties

As a representative example, the UV-Visible absorption spectra of the pyridine and pyrimidine-substituted SBFs are presented in figure 17-left (**4-Ph-SBF** and 2-substituted-SBFs have also been plotted for comparison). SBFs substituted in C4 with either pyrimidine or pyridine show similar absorption spectra with two main bands at ca 297 and 308 nm and a tail around 320 nm. This tail, which translates the π-conjugation extension between the fluorene and the pyridine or the pyrimidine unit, presents different intensities. Thus, in the pyridine series, the authors report that the tail intensity depends on the position of the nitrogen atom. This feature indicates that more intense π-conjugation occurs between fluorene and pyridine units following the sequence **4-2Py-SBF > 4-4Py-SBF > 4-3Py-SBF**. In the case of **4-5Pm-SBF**, the tail presents an almost identical intensity than that of **4-2Py-SBF**. The PHC analogue **4-Ph-SBF** presents a less intense tail (Figure 17 left, black line), compared to pyridine-substituted SBFs. This feature has been correlated to the larger angle formed between the fluorene and the phenyl in C4 in **4-Ph-SBF** (higher than 51.2°) than between the fluorene and the pyridine in C4 in **4Py-SBF** (42.2 °), Figure 16. Compared to **4-Ph-SBF** (ΔE^{opt}: 3.82 eV), **4-3Py-SBF**, **4-2Py-SBF**, **4-4Py-SBF** and **4-5Pm-SBF** possess a slightly narrower optical gap ΔE^{opt} ie 3.81, 3.80 and 3.75 eV and 3.72 eV *resp.* (Table 3). The authors assign this gap contraction to the decrease of the LUMO energy levels induced by the electron withdrawing pyridine or pyrimidine ring (see electrochemistry below). The 2-substituted SBFs, due to their extended conjugation, display a shorter ΔE^{opt} (3.70 eV for **2-4Py-SBF** and 3.66 eV for **2-5Pm-SBF**) compared to their 4-substituted analogues.

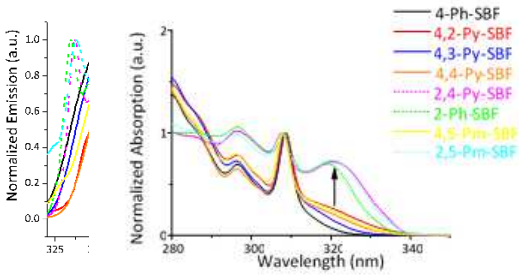

Figure 17. Left: UV-vis absorption and right: emission spectra of SBF derivatives (in cyclohexane).

The electrochemical investigations have shed light on the impact of electron-withdrawing groups in position 4 of a SBF core (cyclic voltammetry samples are provided in Figure 18).[71] The first oxidation of **4-4Py-SBF** and **4-5Pm-SBF** (Figure 18 right) is reported at nearly the same potential than that of **4-Ph-SBF** (1.69 ± 0.1 V). Thus, the incorporation of the pyridine or pyrimidine units at C4 of the SBF core has almost no influence on the HOMO energy levels. Indeed, the HOMOs are reported to lye at -5.88 eV for all the pyridine isomers **4-4Py-SBF**, **4-3Py-SBF** and **4-2Py-SBF**[71] and at -5.97 eV for **4-5Pm-SBF**,[82] compared to -5.95 eV for **4-Ph-SBF**.[81] On the contrary, the electrochemical reduction of **4-4Py-SBF** and **4-5Pm-SBF** (Figure 18 left) is reported at less negative potentials (-2.48 and -2.37 V *resp.*, in THF) than the reduction of **4-Ph-SBF** (-2.64 V, in DMF). This leads to LUMO levels lying at -2.11 eV for **4-4Py-SBF**, at -2.10 eV for **4-2Py-SBF**, at -2.01 eV for **4-3Py-SBF**[71] and at -2.23 eV for **4-5Pm-SBF**,[82] being hence deeper compare to that of **4-Ph-SBF** (LUMO: -1.95 eV).[81] The decrease of the LUMO energy level induced by the pyridyl ring is slightly less pronounced than that of the pyrimidine ring translating the different electron-withdrawing force of these two heterocycles, the latter being stronger than the former. Thus, incorporation of electron-withdrawing pyridine and pyrimidine in C4 of the SBF core has almost no influence on the HOMO energy levels but a significant impact on the LUMO energy levels. This is an important feature in the electrochemistry of 4-substituted SBFs.

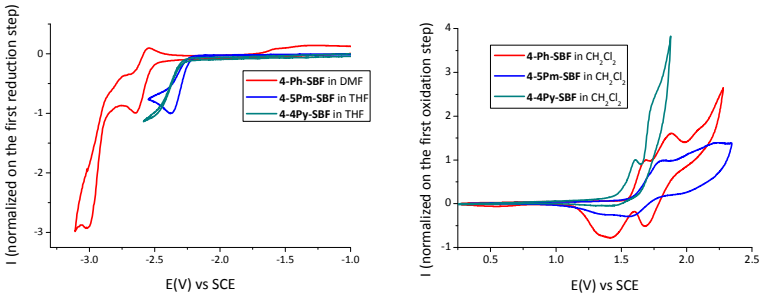

Figure 18. Cyclic voltammetry in reduction (left, recorded in DMF or THF + 0.1 M Bu_4NPF_6) and in oxidation (right, recorded in CH_2Cl_2 + 0.2 M Bu_4NPF_6) of **4-Ph-SBF** (red line), **4-5Pm-SBF** (blue line) and **4-4Py-SBF** (green line). The current is normalized at the first oxidation or reduction step. (Pt disk electrode Ø1 mm, 100 mV/s).

4-substituted SBFs, as already indicated in part 4, present structureless and large emission spectra centred herein at 370 nm for **4-2Py-SBF**, 363 nm for **4-3Py-SBF**, 365 nm for **4-5Pm-SBF** and 369.5 nm for **4-4Py-SBF**, red shifted compared to the emission of **4-Ph-SBF** (358 nm) (figure 17, right).[71, 81] The presence of a pyridyl or pyrimidine unit instead of the phenyl ring induces a bathochromic shift of the emission. The authors have also pointed out that the emission maxima follow the same sequence than that described above in absorption for the intensity of the tail at *ca* 320 nm, indicating that it is directly linked to the intensity of the π-conjugation.

4-2Py-SBF with a Φ_{sol} of *ca* 0.17 and lifetime of 3.88 ns appears clearly less emissive than **4-3Py-SBF**, **4-4Py-SBF** and **4-Ph-SBF** with Φ_{sol} of 0.40, 0.40 and 0.42 and lifetimes of 3.89, 3.80 and 4.20 ns respectively (Table 3). 2-substituted SBFs, **2-4Py-SBF** and **2-Ph-SBF**, show relatively higher Φ_{sol} (0.55 and 0.87) and much shorter lifetimes (1.03 ns and 1.56 ns). Oppositely to pyridine-substituted SBFs, pyrimidine-substituted SBFs shows a quenching of fluorescence with very low Φ_{sol} of 0.04 and 0.02 and lifetimes of 0.61 ns and 0.44 ns for **4-5Pm-SBF** and **2-5Pm-SBF**, respectively.[82] The cause of this quenching is assigned by the authors to the presence of the aromatic NCHN fragment in the 5-pyrimidine unit, which has a strong impact on the deactivation rates of the excited state. Indeed, they report for pyrimidine substituted derivatives **4-5Pm-SBF** and **2-5Pm-SBF** a lower radiative rate constant k_r (6.6×10^7 and 4.6×10^7 s^{-1} *resp.*) and a much higher non-radiative rate constant k_{nr} (1.6×10^9 and 2.2×10^9 s^{-1} *resp.*) compared to phenyl-substituted derivatives **4-Ph-SBF** and **2-Ph-SBF** (k_r of 1.0×10^8 and 5.6×10^8 s^{-1} *resp.* and k_{nr} of 1.4×10^8 and 8.3×10^7 s^{-1} *resp.*).

4-POPh$_2$-SBF and its isomer **2-POPh$_2$-SBF** are herein particular cases. Indeed the tetrahedral geometry of the phosphorus atom insures an efficient conjugation break between the fluorene and the diphenyl-phosphine oxide unit. UV-vis absorption spectra display two absorption bands at 308/322 nm for **4-**

$POPh_2$-SBF[116] and at 308/316 nm for **2-$POPh_2$-SBF**.[116] The band at 308 nm, previously observed for other SBF based compounds, corresponds to π-π* transitions involving the fluorene.[91] The authors do not provide any explanation regarding the nature of the second absorption band red shifted by 6 nm from **2-$POPh_2$-SBF** (316 nm) to **4-$POPh_2$-SBF** (322 nm). The substitution in position 4 in **4-$POPh_2$-SBF** and in position 2 in **2-$POPh_2$-SBF** provides (i) very similar HOMO energy levels (-6.57 *vs* -6.55 eV *resp.*) and (ii) different LUMO energy levels (-2.82 *vs* -2.73 eV *resp.*). The emission spectra of both molecules are almost the same with a large and unresolved band recorded with a maximum at 339 nm and 346 nm for **2-$POPh_2$-SBF** and **4-$POPh_2$-SBF** *resp*.[116] One can note that the emission spectrum of **2-$POPh_2$-SBF** is surprisingly not resolved.

The absorption spectrum of **2,7-DiCbz-SBF-4'-$POPh_2$** (figure 19, left) is different than the others described in this review due to its substitution on both fluorenes.[53] Indeed, due to the presence of the two carbazole units, **2,7-DiCbz-SBF-4'-$POPh_2$** possesses an identical spectrum than that of its constituting building block 2,7-bis-carbazol-9-yl-9,9'SBF (**Spiro-2CBP**)[117] (λ_{max}= 349 nm, ΔE^{opt}=3.41 eV). The absorption bands at low energy have been assigned by the authors to transitions implying the carbazole/fluorene/carbazole fragment. The phosphine oxide in position 4' has hence a limited influence on the optical properties.

The HOMO energy level of **2,7-DiCbz-SBF-4'-$POPh_2$** is evaluated at -5.51 eV by electrochemistry (Figure 19, right),[53] largely higher than that of **SBF** (-5.94 eV)[81] due to the substitution with the two carbazole fragments in C2/C7. The first electron transfer is indeed assigned by the authors to the 'carbazole/fluorene/carbazole' fragment. The cyclic voltammetry of **4-$POPh_2$-SBF** in the same experimental conditions leads to an HOMO level of -6.00 eV.[53] Thus, the HOMO level of **4-$POPh_2$-SBF** is very deep, even slightly deeper than that of **SBF** (-5.94 eV), indicating the slight influence of the phosphine oxide on the fluorene oxidation. Through cathodic explorations, the cyclic voltammetries of **2,7-DiCbz-SBF-4'-$POPh_2$** and of **4-$POPh_2$-SBF** are reported similar leading to the same LUMO energy levels, -2.10 eV. The electrochemical gaps (ΔE^{el}) have been evaluated at ca 3.41 eV for **2,7-DiCbz-SBF-4'-$POPh_2$** and at ca 3.90 eV for **4-$POPh_2$-SBF**. Thus, in **2,7-DiCbz-SBF-4'-$POPh_2$**, the authors state that the main electronic properties are driven by the carbazole/fluorene/carbazole moiety and that the withdrawing effect of the phosphine oxide is weak. This is the consequence of the π-conjugation disruption caused by this sterically hindered linkage and by the tetrahedral geometry of the phosphorus atom. As ΔE^{el} of **SBF** is of 4.05 eV, the C4-substitution of **4-$POPh_2$-SBF** reduces the gap by only 0.15 eV (mainly by decreasing the LUMO level) highlighting the interest of this position to keep a wide gap.

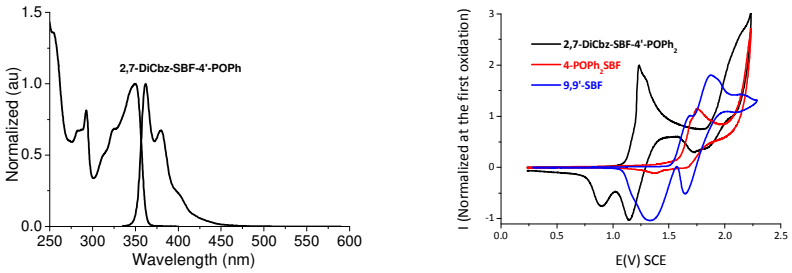

Figure 19. Left: UV-vis absorption and emission spectra of **2,7-DiCbz-SBF-4'-$POPh_2$** (cyclohexane). Right: Cyclic voltammetry (Pt disk electrode Ø1 mm, 100 mV/s, CH_2Cl_2 0.2 M Bu_4NPF_6) in oxidation of **9,9'-SBF** (blue line), **4-$POPh_2$-SBF** (red line) and **2,7-DiCbz-SBF-4'-$POPh_2$** (black line).

2,7-DiCbz-SBF-4'-$POPh_2$ exhibits a well-defined emission spectrum (cyclohexane, λ_{max}= 362/380 nm, Figure 19, left). This behaviour is different to the other 4-substituted SBFs due to the presence of the two carbazole fragments. In addition, **2,7-DiCbz-SBF-4'-$POPh_2$** is a very efficient violet-blue fluorophore with a high Φ_{sol} of 0.78 in solution (quinine sulphate as reference) indicating few non-radiative pathway from S_1 to S_0, and further few intersystem crossing (ISC) from S_1 to T_1 as described below.
The E_T of all these dyes have been evaluated from the emission spectra at 77K. **4-3Py-SBF** and **2-4Py-SBF** respectively possess the highest and lowest E_T in the pyridine series (2.79 eV and 2.58 eV *resp.*)

assigned to the different substitution position (C4 *vs* C2). It should be mentioned that **4-2Py-SBF** (E_T=2.74 eV) possesses the most intense phosphorescence whereas **2-4Py-SBF** (E_T=2.58 eV) possesses the less intense one, translating different efficiencies in term of ISC between S_1 and T_1.[71] Interestingly, the authors correlated these features to the quantum yields Φ_{sol}, **2-4Py-SBF** possessing the highest Φ_{sol} (55%) and the lowest E_T (2.58 eV) and **4-2Py-SBF** possessing the lowest Φ_{sol} (17%) and the highest E_T (2.79 eV).[71] In the pyrimidine series, there is the same amplitude of ca 0.17 eV between the 4-substituted isomer (E_T=2.75 eV for **4-5Pm-SBF**) and its 2-substituted isomer (E_T=2.58 eV for **2-5-Pm-SBF**).

Table 3. Selected electronic and physical data of 2- and 4-SBFs incorporating electron-widrawing groups (**4-Ph-SBF** and **2-Ph-SBF** are also presented for comparison purpose).

	4-Ph-SBF [81]	**2-Ph-SBF** [81]	**4-2Py-SBF** [71]	**4-3Py-SBF** [71]	**4-4Py-SBF** [71]	**2-4Py-SBF** [71]	**4-5Pm-SBF** [82]	**2-5Pm-SBF** [82]	**2,7-DiCbz-SBF-4'-POPh$_2$** [53]	**4-POPh$_2$-SBF**[116,53]
$\lambda_{max,abs}$ (nm)	297, 308 [a]	297, 308, 319 [a]	297, 308 [a]	297, 308 [a]	297, 308 [a]	297, 308, 321 [a]	297, 308, 318 [a]	296,308, 320 [a]	292,349 [a]	308, 322[116,53]
ΔE^{opt}	3.82 [a]	3.70 [a]	3.80 [a]	3.81 [a]	3.75 [a]	3.70 [a]	3.72 [a]	3.66 [a]	3.41 [a]	3.75[116,53]
$\lambda_{max,fluo}$ solution (nm)	358 [a]	335, 351 [a]	370 [a]	363 [a]	369 [a]	337,354, 370 [a]	298, 311 [a]	338, 355 [a]	362,380 [a]	346
$\lambda_{max,fluo}$, thin film (nm) [b]	363	343, 359	366	365	377	375, 425	365	355, 366	-	353[116]
$\lambda_{max,phosphor}$ (77K) (nm)	447 [d]	483 [d]	448 [d]	444 [d]	451 [d]	480 [d]	372 [e]	480 [e]	469	-
E_T (eV)	2.77 [d]	2.56 [d]	2.76 [d]	2.79 [d]	2.74 [d]	2.58 [d]	2.75 [e]	2.58 [e]	2.64	2.78[116]
Φ_{sol} (%) [c]	42	87	17	40	40	55	0.04	0.02	0.87	-
Fluorescence lifetime (ns) [a]	4.2	1.56	3.88	3.89	3.80	1.03	0.61	0.44	4.6	-
Radiative rate constant (k_r) (10^8s)	1.00	5.58	0.44	1.03	1.05	5.34	0.66	0.46	6.4	-
Non-radiative rate constant (k_{nr}) (10^8s)	1.38	0.83	2.14	1.54	1.58	4.37	16	22	1.8	-
HOMO [f]	-5.95	-5.88	-5.88	-5.90	-5.88	-5.78	-5.97	-5.96	-5.51	-6.57[116] -6.00[53]
LUMO [f]	-1.95	-2.10	-2.12	-2.01	-2.11	-2.26	-2.23	-2.30	-2.10	-2.82[116] -2.10[53]
T_d [g]	254	238	242	220	217	181	277	242	426	297[53]
T_g [h]	76	78	81	81	84	92	85	94	193	127[116]

[a] in cyclohexane [b] from a THF solution at 10g/L [c] calculated from a quinine sulfate solution in 1N sulfuric acid solution , [d] in 2-Me-THF, [e] in a methylcyclohexane/2-methylpentane mixture (1:1), [f] from Cyclic Voltammetry, [g] from TGA, [h] from DSC. i. different HOMO/LUMO values are found in literature for this compound

Thus, compared to the E_T of **SBF** (2.87 eV),[81] the substitution by the 3-pyridyl ring (E_T: 2.79 eV) less affects the E_T than the substitution by the 5-pyrimidyl ring (E_T: 2.75 eV)[82] or by the 4- or 2-pyridyl rings (E_T: 2.74 or 2.76 eV, *resp.*), Table 3. The case of **4-POPh$_2$-SBF** is somewhat particular as the phosphorus insures a π-conjugation breaking and the E_T is reported by Lee et al. at 2.78 eV.[116] Due to its high Φ_{sol} of 0.78 in solution, the ISC is not preferred in **2,7-DiCbz-SBF-4'-POPh$_2$** and the phosphorescence contribution is very weak. The opposite was observed above for the pyridine substituted SBFs: low quantum yield and high phosphorescence contribution.[71] Thus, **2,7-DiCbz-SBF-4'-POPh$_2$** presents an E_T of 2.64 eV. The triple substitution of the SBF core in C2/C7 and C4' and the spatial separation of the substituents *via* the spiro bridge only leads to an E_T decrease of 0.23 eV compared to non-substituted **SBF** (E_T= 2.87 eV), remaining high enough to be used as host for green PhOLEDs but not for blue ones.

Thermal properties

T_d of 4-substituted-pyridine SBFs, **4-4Py-SBF**, **4-3Py-SBF** and **4-2Py-SBF**, lie in a small range between 217°C and 242°C, the 2-pyridyl ring leading to the more stable molecule.[71] The T_d are however lower

than that of **4-Ph-SBF** (254 °C). Similarly, T_d of **2-4Py-SBF** is evaluated at 181°C lower than that of **2-Ph-SBF** (238 °C). The substitution of the SBF core by a pyridyl unit instead of a phenyl unit leads then to less thermally stable compounds. Pyrimidine has the opposite effect with **4-5Pm-SBF** possessing a higher T_d (277°C) than that of **4-Ph-SBF**, showing the interest of the incorporation of a pyrimidine unit in C4.

Thus, the substitution position has an influence on the T_d, with an increase of T_d of 16°C from **2-Ph-SBF** to **4-Ph-SBF**, of 35 °C from **2-5Pm-SBF** to **4-5Pm-SBF** and of 36 °C from **2-4Py-SBF** to **4-4Py-SBF**. This T_d increase was however not observed for the couple **2,2'-(SBF)$_2$** (367°C)/**4,4'-(SBF)$_2$** (360°C), part 4. The pyridyl substituent nevertheless has a positive influence on the T_g. Indeed, T_g of **4-4Py-SBF**, **4-3Py-SBF** and **4-2Py-SBF**, lye between 81 and 84°C, being higher than that of **4-Ph-SBF**[81] (76°C). The T_g of **2-4Py-SBF** (92 °C) is also higher than that of **2-Ph-SBF**[82] (78°C). Thus, independently of the substitution (C2 or C4), pyridyl-substituted compounds always possess slightly higher T_g than their phenyl analogues. The same conclusion is drawn for pyrimidine-substituted SBFs, which T_g is higher than that of their phenyl substituted parent (T_g of **4-5Pm-SBF** 85°C *vs* T_g of **4-Ph-SBF** 76°C and T_g of **2-5Pm-SBF** 94°C *vs* T_g of **2-Ph-SBF** 78°C). The authors state that these higher T_g are the consequence of stronger intermolecular interactions due to CH···N hydrogen bonding interactions.[71]

T_d of **4-POPh$_2$-SBF** is reported at 297 °C,[53] being higher than those exposed above, meaning that the introduction of phosphine oxide on C4 increases the T_d. The T_d of **2,7-DiCbz-SBF-4'-POPh$_2$**[53] occurs at the very high temperature of 426 °C significantly higher than those exposed above. This is caused by the increase of molecular weight and by the twisted structure of this molecule. In DSC, T_g of **2,7-DiCbz-SBF-4'-POPh$_2$** is reported at the very high temperature of 193°C, strongly higher than those reported for **4-POPh$_2$-SBF** (127 °C)[116] and for the other 4-substituted SBFs exposed above.[69, 71, 118] This means that the substitution on the two fluorenes is highly beneficial to increase the T_g. The T_g of **4-POPh$_2$-SBF** is nevertheless significantly higher than that of its regioisomer **2-POPh$_2$-SBF** (96°C)[116] indicating that the phosphine oxide position has an important influence on the thermal properties. This result is nevertheless different to those above exposed in the **4-Ph-SBF/2-Ph-SBF** or in the **4-4Py-SBF/2-4Py-SBF** or in the **4-5Pm-SBF/2-5Pm-SBF** series for which the T_g decreases when the substituent moves from the 4 to the 2-position, highlighting the difficulty to draw clear trends.

Phosphorescent OLEDs

The PhOLED structure using pyridyl- or pyrimidine-substituted SBFs as host is the same than that reported for **4-Ph-SBF** and the performance of the devices can be hence directly compared (ITO/CuPc(10nm)/ NPB(40nm)/TCTA(10nm)/Host:dopant(20nm)/TPBi(40nm)/LiF(1.2nm)/Al(100nm)). All the green devices using pyrimidine or pyridine based materials as host, present better performances (12.7<EQE< 15.7%) than those reported for **SBF** (8.5%) and **4-Ph-SBF** (10.4%) table 2).

Table 4. Performance of green (Ir(ppy)$_3$) devices.[a]

	V_{on}(V) @ 1 cd/m^2	E.Q.E (%) @ 10 mA/cm^2	CE (cd/A) @ 1 / 10 mA/cm^2	PE (lm/W) @ 1 / 10 mA/cm^2
4-5-Pm-SBF	3.7	13.8	56.6/50.5	25.9/17.9
4-4-Py-SBF	3.4	15.7	63.4/56.8	33.9/23.1
4-3-Py-SBF	3.6	14.9	57.3/55.5	32.3/24.5
4-2-Py-SBF	3.9	12.7	59.0/47.3	31.0/20.0
2-4-Py-SBF	3.3	14.3	56.3/51.9	31.8/22.3
2-5Pm-SBF	3.1	14.2	56.7/51.4	32.6/22.6
2-Ph-SBF	3.9	9.5	39.6/35.2	21.5/15.3
2,7-DiCbz-SBF-4'-POPh$_2$[b]	2.4	6.2 (13.2[c])	45.8[c]/21.5	49.6[c]/12.4
4-POPh$_2$-SBF[b]	3.3	8.1 (13.3[c])	50.2 [c]/30.5	29.8 [c]/9.6

[a] Multiplayer Device structure: ITO/CuPc(10 nm)/NPB(40 nm)/TCTA(10 nm)/Ir(ppy)$_3$:host(10 wt%,20 nm)/TPBi(40 nm)/LiF(1.2 nm)/Al(100 nm).
[b] Single-Layer device structure: ITO/PEDOT:PSS(40 nm)/Host:Ir(ppy)$_3$ (100 nm)/LiF(1.2 nm)/Al(100 nm).
[c]. EQE, CE or PE maximum value

Thus, the device using **4-5Pm-SBF** as host has a V_{on} of 3.7 V and presents a CE of 50.5 cd/A, a PE of 17.9 lm/W, and an EQE of 13.8% (at 10 A/cm^2), strongly higher than that of PHC **SBF** and **4-Ph-SBF** (Table 2).
The green devices using pyridyl-substituted SBFs as host all present similar performances and the best ones are reported for **4-4Py-SBF**. This device emits light at 3.4 V and presents a CE of 56.8 cd/A, a PE of 23.1 lm/W and an EQE of 15.7% (at 10 A/cm^2). PhOLEDs using **4-3Py-SBF** and **4-4Py-SBF** as host present better performance than that using **4-5Pm-SBF**, with V_{on} lowered by 0.1-0.3 V and EQE increased by 1-2%, highlighting that pyridine is more efficient than pyrimidine in such design. However, as the LUMO is more decreased by the introduction of pyrimidine, this parameter cannot be the only involved in the different performance. It should be mentioned that these values are all recorded at 10 mA/cm^2 (values at 1 mA/cm^2 are also provided in Table 4) by the authors and are not maximum values as often reported.

For comparison, the 2-substituted compounds **2-4Py-SBF** and **2-5Pm-SBF** have also been reported as host in identical devices. The EQE (at 10 mA/cm^2) of the device using **2-4Py-SBF** is reported at 14.3% almost identical to that using **2-5Pm-SBF** (14.2%)[82] but strongly higher than that reported for **2-Ph-SBF** (9.5%). There is also a decrease of the V_{on} from 3.9 V for **2-Ph-SBF** to 3.3 V for **2-4Py-SBF** and to 3.1 V for **2-5Pm-SBF**. The EQE of **2-4Py-SBF** is nevertheless lower than that of **4-4Py-SBF** (14.3% *vs* 15.7%).

2,7-DiCbz-SBF-4'-POPh$_2$ has been incorporated as host in a very simple single-layer green PhOLED (Ir(ppy)$_3$) with no transporting neither blocking layers. Indeed, simplifying the device architecture to reach single-layer PhOLEDs is an important research field which would be beneficial to decrease the whole cost of PhOLEDs. The architecture is the following : ITO/PEDOT:PSS (40 nm)/Host:Ir(ppy)$_3$(10%) (100 nm)/LiF(1.2 nm)/Al (100 nm). This single-layer PhOLED displays high maximal EQE of 13.2%, maximum CE of 45.8 cd/A and maximum PE as high as 49.6 lm/W (at 0.01 mA/cm², Table 4).[53] The V_{on} is very low (2.4 V), translating an excellent charge injection within the EML. In order to shed light on the effect of the phosphine oxide on the device performance, the authors also have investigated benchmark devices using **4-POPh$_2$-SBF** as host in a similar device architecture. Single-layer PhOLED using **4-POPh$_2$-SBF** as host displays an EQE as high as that of **2,7-DiCbz-SBF-4'-POPh$_2$**-based PhOLED, ie 13.3%, this performance indicating the strong influence of the phosphine oxide fragment in the PhOLED performance. However, due to the deeper HOMO level of **4-POPh$_2$-SBF** (-6.00 eV), the green single-layer PhOLED displays a higher V_{on} of 3.3 V, *ca* 1V higher than that using **2,7-DiCbz-SBF-4'-POPh$_2$** as host (HOMO level:-5.53 eV) due to a better charge injection in the latter than in the former. The performance of **2,7-DiCbz-SBF-4'-POPh$_2$** was among the highest reported for green single-layer PhOLEDs.[53]
The electron and hole mobility of a host influence the performance of a device and especially of a single-layer device. The authors have evaluated the charge carriers properties of **2,7-DiCbz-SBF-4'-POPh$_2$** by the Space Charge Limited Current method.[53] There is around one order of magnitude between the hole mobility (μ_h: 8.5×10^{-7} cm^2/V.s) and the electron mobility (μ_e: 4.2×10^{-8} cm^2/V.s) which is an important feature for a well balance within the OLED.[53] This feature is correlated by the authors to the high performance of the **2,7-DiCbz-SBF-4'-POPh$_2$** green single layer device. The determination of the electron mobilities of **4-POPh$_2$-SBF** and **2-POPh$_2$-SBF** using electron only devices is also reported in literature.[116] μ_e values of 7×10^{-4} cm^2/V.s for **4-POPh$_2$-SBF** and 5×10^{-4} cm^2/V.s for **2-POPh$_2$-SBF** indicate a slight modulation induced by the position of the phosphine oxide fragment on the SBF cores.

Table 5. Performance of blue (FIrpic) devices.

	V_{on} (V) @1 cd/m^2	E.Q.E (%) @10 mA/cm^2	CE (cd/A) @1/10 mA/cm^2	PE (lm/W) @1 / 10 mA/cm^2
SBF[a]	4.0	6.5	20.1/18.7	10.8/7.9
4-Ph-SBF[a]	4.7	6.0	18.4/16.7	8.5/6.1
4-5Pm-SBF[a]	4.1	5.0	15.2/14.5	7.9/5.7
4-4Py-SBF[a]	4.3	5.1	16.1/14.6	8.3/5.9
4-3Py-SBF[a]	4.7	4.9	16.2/14.2	7.5/5.1

4-2Py-SBF[a]	5.0	3.9	10.9/10.4	4.8/3.6
2-4Py-SBF[a]	4.8	0.2	0.7/0.6	0.4/0.3
4-POPh$_2$-SBF[b]	-	17.5[c]	35.6[c]	24.7[c]
4-POPh$_2$-SBF[d]	-	17.2[e]	35.3[e]	26.0[e]

[a]Device structure: ITO/CuPc(10 nm)/NPB(40 nm)/TCTA(10 nm)/FIrpic:host(20 wt%, 20 nm)/TPBi(40 nm)/LiF(1.2 nm)/Al(100 nm).
[b]Device structure: ITO/PEDOT:PSS(60 nm)/NPB(20 nm)/mCP(10 nm)/FIrpic:**4-POPh$_2$-SBF**(ca 10/11 wt%,30 nm)/**4-POPh$_2$-SBF**(25 nm)/LiF(1 nm)/Al(100 nm)
[c]EQE, CE or PE @300 cd/m^2.
[d]Device structure:ITO/PEDOT:PSS(60nm)/NPB(20nm)/mCP(10nm)/FIrpic:**4-POPh$_2$-SBF**(10%,30nm)/BCP(5nm)/Alq$_3$(20nm)/LiF(1nm)/Al (100nm)
[e]EQE, CE or PE @200 cd/m^2.

The 4-substituted SBFs incorporating electrowithdrawing fragments have also been used as host for the sky blue emitter FIrpic (Table 5). The moderate performances of the resulting PhOLEDs based on the three pyridines are in the same range with however slightly better performances for **4-3Py-SBF** and **4-4Py-SBF**, indicating that 3-pyridine and 4-pyridine rings are the most efficient pyridyl regioisomers for PhOLEDs (in both green and blue). At 10 mA/cm^2, an EQE of 5.1% and a V$_{on}$ of 4.3 V are reported for **4-4Py-SBF** and an EQE of 4.9% and a V$_{on}$ of 4.7 V are reported for **4-3Py-SBF**. The blue devices using **4-2Py-SBF** as host display lower performance than that using the precedent isomers (EQE = 3.9%/V$_{on}$ =5.0 V) following the same trend observed for the green devices. The blue devices using **4-5Pm-SBF**[82] (V$_{on}$= 4.1 V/ EQE=5%) present similar performances than those reporded for **4-4Py-SBF**.

4-POPh$_2$-SBF was also incorporated as host for FIrpic in a multilayer PhOLED with two different architectures:ITO/PEDOT:PSS(60nm)/NPB(20nm)/mCP(10nm)/**4-POPh$_2$-SBF**:FIrpic(10%)(30nm)/BCP (5nm)/Alq$_3$(20nm)/LiF(1nm)/Al(100nm) and ITO/PEDOT:PSS (60nm)/NPB(20nm)/ mCP(10nm)/**4-POPh$_2$-SBF**:FIrpic (10%)(30nm)/**4-POPh$_2$-SBF**(25nm)/LiF(1nm)/Al (100nm).[116] In the first architecture, **4-POPh$_2$-SBF** is only used as host for FIrpic and in the second, it has a double role, host for FIrpic and electron transporting layer. With the first architecture, the **4-POPh$_2$-SBF-**based PhOLED displays a high maximum EQE of 17.2%, maximum CE and PE of 35.3 cd/A and 26.0 lm/W. This performance is better than that reported for its isomer **2-POPh$_2$-SBF** in an identical device configuration (EQE: 15.6%).[116]
Using the second device architecture, in which **4-POPh$_2$-SBF** is used both as host in the EML and as electron transport layer, higher performances were obtained (EQE of 17.5%, CE of 35.6 cd/A and PE of 24.7 lm/W). Thus, phosphine oxide based materials display strongly higher performance than that of pyridine or pyrimidine based materials, highlighting the remarkable influence of this core.

6. 4-substituted SBF incorporating electron-donating units.

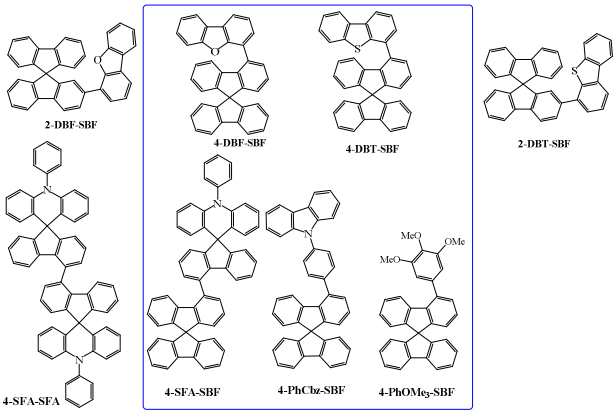

Figure 20: Electron rich molecules based on a 4-substituted SBF scaffold (and their 2-substituted analogues)

To the best of our knowledge, only five examples of 4-substituted SBFs incorporating electron-donating fragments have been reported as host in PhOLEDs (figure 20). **4-DBF-SBF** (4-(9,9'-spirobi[9*H*-fluoren]-2-yl)-dibenzofuran) reported by Lee et al. in 2012 is built on a SBF backbone possessing in C4 a

dibenzofuran fragment.[118] In 2013, the same group has reported the incorporation of a dibenzothienyl core in C4 of a SBF unit leading to **4-DBT-SBF** (4-(9,9'-spirobi[9*H*-fluoren]-4-yl)-dibenzothiophene).[119] The group of Ma has reported in 2014 the incorporation in C4 of a spiro-fluorene-phenylacridine **4-SFA-SBF** (10-phenyl-4'-(9,9'-spirobi[9*H*-fluoren]-4-yl)-spiro[acridine-9(10*H*),9'-[9*H*]fluorene])[120] and following a similar design, also has reported a dimer of spiro-fluorene-phenylacridine linked by their C4 in **4-SFA-SFA** (10,10'-diphenyl-4',4''-bispiro[acridine-9(10*H*),9'-[9*H*]fluorene]). Our group has reported in 2017 two other dyes incorporating electron-rich fragments in C4 either a trimethoxybenzene in **4-PhOMe$_3$-SBF** (4-(3,4,5-trimethoxyphenyl)-9,9'-spirobi[fluorene]) or a phenyl N-carbazole in **4-PhCbz-SBF**).[95] This last example appears particularly singular as it possesses different properties than those reported in this review.

Synthesis

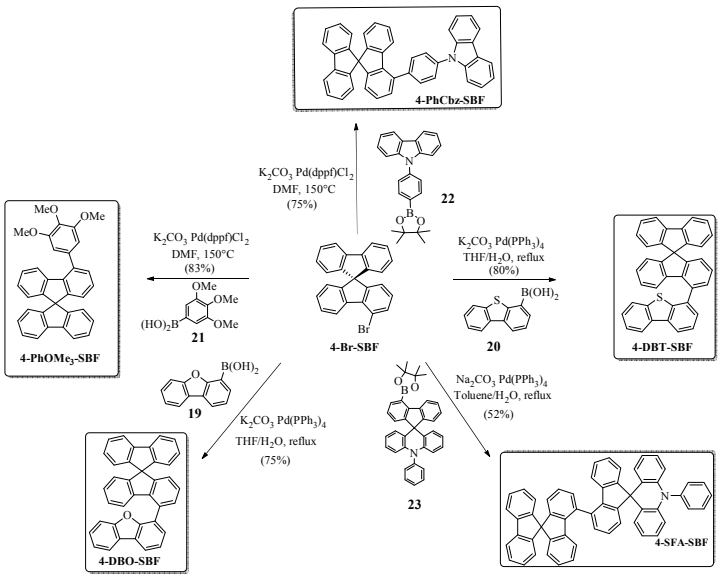

Figure 21. Synthesis of **4-DBF-SBF**,[118] **4-DBT-SBF**,[119] **4-PhOMe$_3$-SBF**,[95] **4-PhCbz-SBF**[95] and **4-SFA-SBF**[120]

As depicted figure 21, **4-DBF-SBF** and **4-DBT-SBF** have been synthesized by the group of Liao from Suzuki coupling of **4-Br-SBF** with respectively 4-(dibenzofuranyl)boronic acid **19** (Yield=75%) or 4-dibenzothienylboronic acid **20** (yield=80%). Similarly, **4-PhOMe$_3$-SBF** and **4-PhCbz-SBF** were also synthesized with high yields (83 and 75% respectively) from **4-Br-SBF** and 3,4,5-trimethoxyphenylboronic acid **21** or 9H-carbazole-9-(4-phenyl) boronic acid pinacol ester **22** respectively. The **4-SFA-SBF** has also been synthesized in a similar manner, through the coupling of **4-Br-SBF** with the spirofluorene phenylacridine derivative **23** (yield=52%).

Structural Properties

No X-ray data have been reported neither for **4-DBF-SBF**[118] nor for **4-DBT-SBF**.[119] However, for the 2-substituted derivatives, **2-DBF-SBF** and **2-DBT-SBF**, angles as high as 53.5° between the two linked phenyl units have been reported by the authors from X-Ray data. These large dihedral angles of 2-substituted SBFs suggest that the 4-substituted SBFs should even possess larger angles. Molecular modelling of **4-DBF-SBF** and **4-DBT-SBF** confirms this feature revealing large dihedral angles of 63.9° and 76.1°, suggesting an intense π-conjugation breaking between the fluorene and either the dibenzofuran or the dibenzothiophene. Moreover, molecular modelling performed for **4-SFA-SBF** and **4-SFA-SFA** reveals a larger angle close to 90° between the two ortho connected fluorene cores.[120]

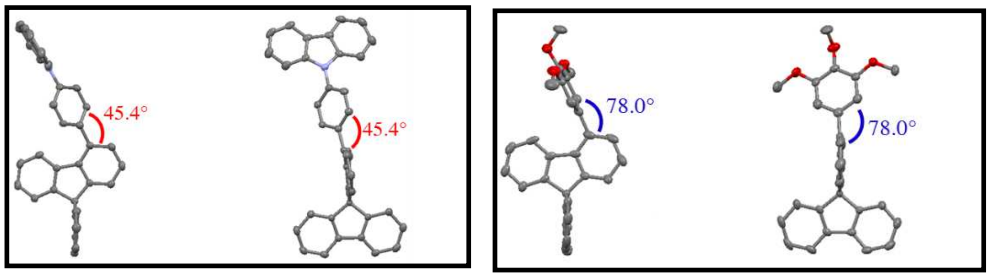

Figure 22. Molecular structures of **4-PhCbz-SBF** (left) and of **4-PhOMe$_3$-SBF** (right) from X-Ray data.[95]

The only available X-ray data of 4-substituted SBFs incorporating electron rich fragments are those recently reported for **4-PhCbz-SBF** and **4-PhOMe$_3$-SBF** (Figure 22).[95] Thus, the angle between the mean plane of the fluorene and that of its C4-substituent is reported at 45.4° for **4-PhCbz-SBF** and at 78° for **4-Ph(OMe)$_3$-SBF**. Despite a larger substituent attached, **4-PhCbz-SBF** displays a smaller angle than that

of **4-Ph(OMe)$_3$-SBF**. The authors conclude that the substitution pattern, *i.e. meta/para vs para*, of the pendant phenyl has a stronger impact on the angle than the bulkiness of the substituent itself. Compared to unsubstituted **4-Ph-SBF,**[81] the fluorene/phenyl angle is slightly smaller for **4-PhCbz-SBF** and much larger for **4-Ph(OMe)$_3$-SBF**, translating different π-conjugation breaking. Regarding the deformation of the substituted fluorene, two different cases are reported. First, for **4-PhCbz-SBF**, a strong deformation of the substituted fluorene core, 11.2°, is reported (similar to that of **4-Ph-SBF,** 12.7°).[81] However, it is difficult to rationalize these fluorene foldings since a very small angle of 2.7° is reported for **4-Ph(OMe)$_3$-SBF**.[95]

Electronic properties

The electronic properties of the couples **4-DBF-SBF/2-DBF-SBF** and **4-DBT-SBF/2-DBT-SBF** are similar and in accordance with those exposed above, highlighting the limited influence of the sulphur and oxygen atom on the electronic properties. ΔE^{opt} are reported at 3.52 /3.83 eV for **2-DBF-SBF/4-DBF-SBF**[118] and 3.5/3.7 eV for **2-DBT-SBF/4-DBT-SBF**.[119] The dibenzofuran leads hence to a less extended conjugation compared to dibenzothiophene and hence to a slightly wider ΔE_{opt}. **4-SFA-SBF** and **4-SFA-SFA** also present a main band at 308 nm (fluorene/fluorene transition) giving a wide ΔE^{opt} of 3.93 eV for both compounds.[120] In fluorescence spectroscopy, the classical unresolved band is reported for **4-DBF-SBF**, this band being red shifted by 19 nm compared to that of **2-DBF-SBF** (369 *vs* 350 nm). **4-SFA-SBF** and **4-SFA-SFA** display a similar behaviour with a large band at 380 and 387 nm respectively. However, the couple **4-DBT-SBF/2-DBT-SBF** does not follow this classical trend as **4-DBT-SBF** displays a blue shifted band (355 nm) compared to that of **2-DBT-SBF** (366 nm). Thus, if the band of **4-DBT-SBF** can be seen as classical, that of **2-DBT-SBF** appears surprising. This peculiar feature, surely due to the presence of the dibenzothiophene and/or to its anchoring position on the fluorene core is not detailed by the authors.

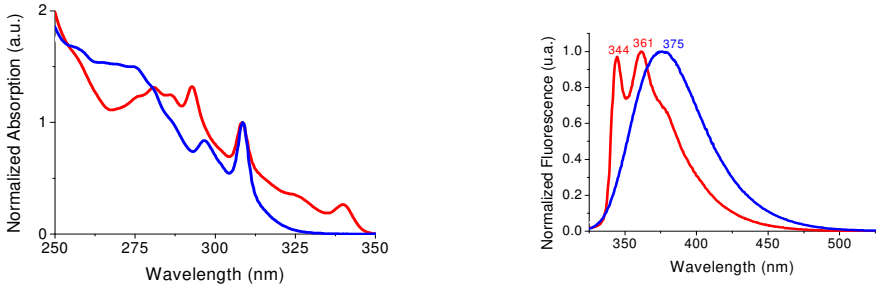

Figure 23. Normalized Absorption (left) and emission (right, λ_{exc} : 309 nm) spectra of **4-PhCbz-SBF** (red lines) and of **4-Ph(OMe)$_3$-SBF** (blues lines) recorded in cyclohexane, C : 10^{-6}M

As presented figure 23, both **4-Ph(OMe)$_3$-SBF** and **4-PhCbz-SBF** present the same absorption band (λ_{max}= 309 nm) similar to that of **SBF** and **4-Ph-SBF** (transitions occurring on the SBF core). For **4-Ph(OMe)$_3$-SBF**, the contribution at 309 nm presents the 'classical' wavelength tail exposed all along this review, leading to a ΔE^{opt} of 3.82 eV (Figure 23-left). As above mentioned with pyridine isomers, this tail possess different intensities translating different coupling intensities between the fluorene and is subsituent.[71] Herein, the intensity of the tail is almost identical between **4-Ph-SBF** and **4-Ph(OMe)$_3$-SBF** showing that the trimethoxy units only have a weak influence on the absorption. This conjugation effect cannot be explored in the case of **4-PhCbz-SBF** because of the presence of an additional band at 340 nm, assigned by the authors to transitions exclusively implying the N-phenyl carbazole fragment (ΔE^{opt} **4-PhCbz-SBF:** 3.58 eV).[95]

As observed for other 4-substituted SBFs (see above), the fluorescence spectrum of **4-Ph(OMe)$_3$-SBF** is structureless (λ= 375 nm, Figure 23-right). The authors noted that the fluorescence spectrum of **4-Ph(OMe)$_3$-SBF** displays the same shape than that of **4-Ph-SBF** but shifted by 17 nm (λ=359 nm). Thus, both molecules possess a very large Stokes shift, which is one of the characteristics of the uncommon fluorescence of 4-substituted SBFs.[69, 70, 81, 88, 116, 118, 119] The authors provide in this work[95] the beginning of an answer. Indeed, the large Stokes shift can found its origin in the significant differences between

the geometries of the ground (S0) and first singlet excited (S1) states observed for both **4-Ph(OMe)$_3$-SBF** and **4-Ph-SBF** through theoretical calculations. The geometry difference between S0 and S1 is also more pronounced for **4-Ph(OMe)$_3$-SBF** than for **4-Ph-SBF** explaining the difference observed in term of Stokes shift. Thus, due to a low rigidity, which allows important rearrangements at the excited state, these two molecules and more generally the 4-substituted SBFs possess large and unresolved fluorescence spectra.

4-PhCbz-SBF appears as a unique example in the 4-substituted SBFs family reported to date as it has not only a well resolved emission spectrum (λ_{max}= 345, 361 nm, Figure 23-right,) but also a small Stokes shift (5 nm). The authors correlate this feature with the very similar geometries of S0 and S1 obtained by molecular modelling.[95] This is a significant difference with **4-Ph(OMe)$_3$-SBF** and **4-Ph-SBF** above mentioned and all the other 4-substituted SBFs. Thus, the presence of the carbazole has a key role in the peculiar fluorescence of **4-PhCbz-SBF** by avoiding molecular rearrangements between S0 and S1. The high rigidity of **4-PhCbz-SBF** could also explain the well resolved fluorescence compared to other 4-substituted SBFs. This is the first rationalization of the peculiar fluorescence of this family of dyes.[95]

Table 6. Selected electronical and physical data for **4-DBF-SBF/2-DBF-SBF**[118] **4-DBT-SBF/2-DBT-SBF,**[119] **4-PhOMe$_3$-SBF**,[95] **4-PhCbz-SBF**,[95] and **4-SFA-SBF/4-SFA-SFA**[120]

	2-DBF-SBF[118]	**4-DBF-SBF**[118]	**2-DBT-SBF**[119]	**4-DBT-SBF**[119]	**4-PhOMe$_3$-SBF**[95]	**4-PhCbz-SBF**[95]	**4-SFA-SBF**[120]	**4-SFA-SFA**[120]
$\lambda_{max,abs}$ (nm)	288, 308,326[a]	279, 308[a]	290,308, 318[a]	286,309[a]	297, 309[g]	293, 309, 340[g]	308[a]	308[a]
$\lambda_{max,fluo}$ solution (nm)	350/366[a]	369[a]	366[a]	355[a]	375[g]	345/361[g]	380[i]	387[i]
$\lambda_{max,phospho}$ (77K) (nm)[b]	490	440	488	441	437	442	437	437
E_T [b,c] (eV)	2.53	2.82	2.49	2.82	2.84	2.81	2.83	2.83
ΔE^{opt} (eV) in solution	3.52	3.83	3.5	3.7	3.82	3.58	3.93	3.93
ΔE^{opt} (eV) in film	3.54	3.79	3.4	3.6	-	-	-	-
T_g (°C)	115	124	122	131	90	127	188	189
T_d (°C)	302	305	318	317	340	410	402	408
HOMO (eV)	-5.83[e]	-6.00[e]	-6.1[d]	-6.3[d]	-5.62[e]	-5.52[e]	-5.33[e]	-5.31[e]
LUMO (eV)	-2.31[e]	-2.17[e]	-2.7[f]	-2.7[f]	-1.91[e]	-1.97[e]	-1.83[h]	-1.81[h]

[a] in DCM [b] in 2-Me-THF solution at 10g/L [c] from first phosphorescent peak (emission spectrum at 77K) in solution , d. from UPS, e. from cyclic voltammetry, f. from HOMO and ΔE^{opt} in film, g. in cyclohexane, h. from HOMO and ΔE^{opt} in solution, i. in toluene

The E_T of all the molecules presented in this part lye in the same short range. Thus, the E_T of **4-Ph(OMe)$_3$-SBF** and **4-PhCbz-SBF** are reported at 2.84 and 2.81 eV respectively, those of **4-DBF-SBF** and **4-DBT-SBF** at 2.82 eV[118] and those of **4-SFA-SBF** and **4-SFA-SFA** at 2.83 eV.[120]

The HOMO/LUMO energy levels are always difficult to compare as not obtained in similar experimental conditions. Thus, the HOMO of **2-DBF-SBF** measured by electrochemistry is lying at -5.83 eV, being 0.17 eV higher than that of **4-DBF-SBF** (-6.00 eV).[118] If one compare with that of **4-Ph-SBF** (-5.95 eV) and that of **2-Ph-SBF** (-5.88 eV), one can note that the trend is identical and translates the π-conjugation interruption in **4-DBF-SBF**. The fact that the HOMO energy level of **4-DBF-SBF** is lower than that of **4-Ph-SBF** (and that of **SBF**, -5.94 eV) may be related to the different experimental conditions. The LUMOs are respectively recorded at -2.31 eV and -2.17 eV for **2-DBF-SBF** and **4-DBF-SBF** translating a similar effect. The HOMOs of **2-DBT-SBF** and **4-DBT-SBF** have been evaluated by Ultraviolet Photoelectron Spectroscopy (UPS) at -6.1 eV and -6.3 eV[119] and the values are hence different to those exposed above. However, a similar trend is found. The HOMO levels of **4-PhCbz-SBF** and **4-Ph(OMe)$_3$-SBF**, determined by cyclic voltammetry, respectively lye at -5.52 eV and at -5.62 eV. These HOMO energy levels are very close to those of their corresponding electron donating fragment, **N-PhCbz** (-

5.59 eV) and **Ph(OMe)$_3$** (-5.67 eV), confirming the significant impact of these building blocks on the HOMO energies.[95] However, the C4 substituted fluorene has a non-negligible influence on the HOMO energy levels as the conjugation is not completely broken. The HOMO energy levels of both **4-PhCbz-SBF** and **4-Ph(OMe)$_3$-SBF** lye ca 0.3/0.45 eV higher than that of **4-Ph-SBF** (and those of **4-DBF-SBF** and **4-DBT-SBF**), due the electron-rich character of the carbazole or the methoxy groups. Thus, the authors state that due to the conjugation disruption at the C4 position of **SBF**, the HOMOs are mainly governed by the electron-rich building blocks with nevertheless an influence of the SBF core.
Finally, in the case of **4-SFA-SBF** and **4-SFA-SFA**, the electron-rich phenylacridine also controls the HOMO levels reported through cyclic voltammetry at -5.31 eV and -5.33 eV respectively.[70] These HOMO levels are very similar to those reported for other spiro compounds incorporating a phenylacridine core.[59-61]

Thermal Properties

The T_g is slightly increased from **2-DBF-SBF** to **4-DBF-SBF** (115 *vs* 124°C) and from **2-DBT-SBF** to **4-DBT-SBF** (122 *vs* 131°C), highlighting a substitution effect, which is nevertheless rather weak. On the other hand, this position effect has almost no impact on the T_d but the nature of the substituent has, the dibenzothiophene fragment leading to higher T_d than dibenzofuran. **4-Ph(OMe)$_3$-SBF** and **4-PhCbz-SBF** respectively present T_g/T_d of 90/340°C and 127/410°C. Thus, the presence of the carbazole core not only significantly modifies the electronic properties but also strongly enhances the physical properties of the resulting material. **4-PhCbz-SBF** displays the highest T_d in this series (410 °C). **4-SFA-SBF** and **4-SFA-SFA** also have excellent thermal properties with T_g/T_d reported at 188/402°C and at 189/408°C respectively. It should be stressed that **4-SFA-SBF** and the PHC dimer **4,4'-(SBF)$_2$** (Figure 7)[70] only differs by the presence of a spiroconnected phenylacridine in the former instead of a spiro connected fluorene in the latter. As **4,4'-(SBF)$_2$** possesses a T_d of 360°C and a T_g of 170°C, one can conclude that switching from fluorene to phenylacridine leads to an enhancement of the thermal properties.

Phosphorescent OLEDs

Table 7. Selected PhOLEDs data for **4-DBF-SBF/2-DBF-SBF**[118] **4-DBT-SBF/2-DBT-SBF,**[119] **4-PhOMe$_3$-SBF**, [95] **4-PhCbz-SBF**,[95] and **4-SFA-SBF/4-SFA-SFA**[120]

	2-DBF-SBF[b]	4-DBF-SBF[b or c]	2-DBT-SBF[b]	4-DBT-SBF[b or c]	4-PhOMe$_3$-SBF[a or d]	4-PhCbz-SBF[a or d]	4-SFA-SBF[e]	4-SFA-SFA[e]
Green Devices with dopant Ir(ppy)$_3$[a] or Ir(ppy)$_2$acac[b]								
EQE (%)[f]	20.2	21.2	15	16.3	20.2	17.5	-	-
CE (cd/A)[f]	59.3	64.4	56.9	62	78	67.9	-	-
PE (Lm/W)[f]	46.1	49.7	33.8	45.9	48.1	45.4	-	-
V_{on} (V)	4.9	4.9	5.3	5.3	4.15	3.7	-	-
Blue Devices with dopant FIrpic								
EQE (%)[f]	-	7.5	-	10.3	9.6	6.7	14	19.1
CE (cd/A)[f]	-	22.2	-	23.5	24.2	18	29.4	41
PE (Lm/W)[f]	-	16.4	-	16.6	13.9	11	30.4	42
V_{on} (V)	-	5.6	-	6.7	4.2	3.75	2.9	2.8

[a] ITO/CuPc (10 nm)/NPB (40 nm)/TCTA (10 nm)/ host:Ir(ppy)$_3$ (9%) (20 nm)/TPBi (40 nm)/LiF (1.2 nm)/Al (100 nm)
[b] ITO/MoO_3 (10 nm)/NPB (35 nm)/TCTA (10 nm)/host:Ir(ppy)$_2$acac (8 wt%, 15 nm)/ TPBi (65 nm)/Liq (20 nm)/Al (100 nm)
[c] ITO/MoO_3(10 nm)/NPB (80 nm/TCTA (5 nm)/host:FIrpic (8% wt%,20 nm)/ TPBi (40 nm)/Liq (2 nm)/Al (100 nm)
[d] ITO/CuPc (10 nm)/NPB (40 nm)/TCTA (10 nm)/ host:FIrpic (20 wt%, 10 nm)/TPBi (40 nm)/LiF (1.2 nm)/Al (100 nm)
[e] ITO/MoO_3 (10 nm)/TAPC (60 nm)/host:FIrpic (10 wt%, 15 nm)/TmpyPBi (35 nm)/LiF (1 nm)/Al (120 nm)
[f] maximum values

PhOLEDs using bis[2-(2-pyridinyl-*N*)phenyl-C](2,4-pentanedionato-O^2,O^4)iridium(III) (Ir(ppy)$_2$acac) as green phosphor were fabricated with **2-DBT-SBF/4-DBT-SBF** and **2-DBF-SBF/4-DBF-SBF**.[118] As the device architectures are identical, the performances can be compared. The architecture is the following ITO/ MoO_3(10nm)/NPB(35nm)/TCTA(10nm)/host:Ir(ppy)$_2$acac(8wt%,15nm)-/TPBi(65nm)/Liq(2nm)/Al (100 nm). **4-DBT-SBF** displays a higher performance than that of **2-DBT-SBF** with an EQE of 16.3% *vs* 15%, CE of 62 *vs* 56.9 cd/A and PE of 45.9 *vs* 33.8 Lm/W. A similar result was

obtained with the couple **2-DBF-SBF**/**4-DBF-SBF**.[118] Indeed, the device using **4-DBF-SBF** as host shows higher performances (EQE of 21.2%, a CE of 64.4 cd/A and a PE of 49.7 Lm/W) than those reported for **2-DBF-SBF** (EQE of 20.2%, a CE of 59.3 cd/A and a PE of 46.1 Lm/W). These performances indicate (i) that 4-substituted SBFs are more efficient than 2-substituted SBFs and (ii) that dibenzofuran is strongly more efficient than dibenzothiophene to host $Ir(ppy)_2acac$ (EQE of 21.2% *vs* 16.3%). With an identical device configuration (but different layer thicknesses, table 7), **4-DBF-SBF** and **4-DBT-SBF** have also been incorporated as host for the sky blue emitter FIrpic. This time, this is **4-DBT-SBF**, which presents the highest efficiency with an EQE of 10.3%, a CE of 23.5 cd/A and a PE of 16.6 Lm/W, **4-DBF-SBF**, displaying a lower performance with an EQE of 7.5%, a CE of 22.2 cd/A and a PE of 16.4 Lm/W. The V_{on} of both devices are relatively high, 5.6 V for **4-DBF-SBF** and 6.7 V for **4-DBT-SBF**. This difference in term of host performance between green and blue phosphors highlights the strong difficulty to rationally design host materials for PhOLEDs.

4-Ph(OMe)$_3$-SBF and **4-PhCbz-SBF** have also been studied in similar devices: ITO/CuPc(10 nm)/NPB(40 nm)/TCTA(10 nm)/Host:$Ir(ppy)_3$(9 wt%)(20 nm)/TPBi(40 nm)/LiF(1.2 nm)/Al(100 nm) for green devices and ITO/CuPc(10 nm)/NPB(40 nm)/TCTA(10 nm)/Host:FIrpic(19 wt%)(20 nm)/TPBI (40nm)/LiF(1.2nm)/ Al(100nm) for blue devices. With green emitter $Ir(ppy)_3$, **4-PhCbz-SBF** presents a maximum EQE of 17.5%, a CE of 67.9 cd/A and a PE of 45.4 Lm/W. With sky blue emitter FIrpic, the performance of **4-PhCbz-SBF** decreases with a maximum EQE of 6.7%, a CE of 18 cd/A and a PE of 11 Lm/W. **4-Ph(OMe)$_3$-SBF** displays higher performance both in green and blue devices. Thus, with $Ir(ppy)_3$, a maximum EQE of 20.2% is reached with a CE of 78 cd/A and a PE of 48.1 Lm/W. With FIrpic, the EQE is reported at 9.6% (CE of 24.2 cd/A and PE of 13.9 Lm/W). Thus, the presence of the strong electron-donating trimethoxyphenyl group leads to efficient devices.

The best blue device performances in the series have been obtained using **4-SFA-SBF** as host for FIrpic (EQE=14%, CE= 29.4 cd/A and PE= 30.4 Lm/W).[70] This high performance is mainly due to the electron-rich phenylacridine core which facilitates the holes injection. This feature is confirmed thanks to the higher performances reported for **4-SFA-SFA** as host (EQE: 19.1 %, CE 41 cd/A and PE 42 Lm/W), clearly signing the efficiency of the phenylacridine fragment to host FIrpic.[70]

7. Other dyes based on a 4-substituted SBF backbone

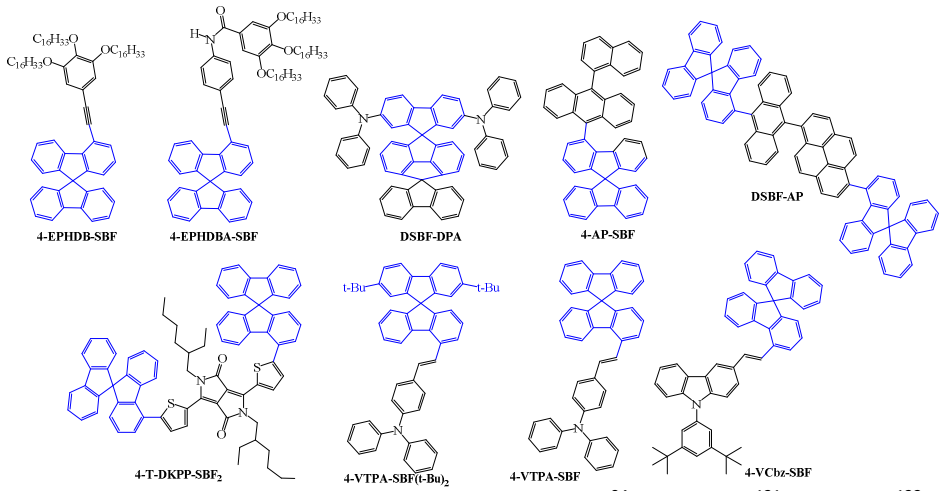

Figure 24. Molecular structures of **4-EPHDBA-SBF** and **4-EPHDB-SBF**,[94] **DSBF-DPA**,[121] **4-AP-SBF**,[122] **DSBF-AP**,[123] **4-T-DKPP-SBF$_2$**,[124] **4-VTA-SBF(t-Bu)$_2$**,[125] **4-VTPA-SBF** and **4-VCbz-SBF**[126]

Before concluding, it is important to mention that some other dyes incorporating the 4-substituted SBF scaffold have been reported for other applications than hosting phosphors in PhOLEDs. Indeed, recent works also have hilighted the potential of this platform for other applications such as blue emissive materials,[94, 123] blue dopant (guest) in fluorescent OLEDs,[125, 126] host in blue fluorescent OLEDs,[122] hole transport material for green PhOLEDs[121] or hole transport material for solar cells.[124] To conclude, we wish to mention these dyes in order to well reflect the state of the art (Figure 24).

Synthesis

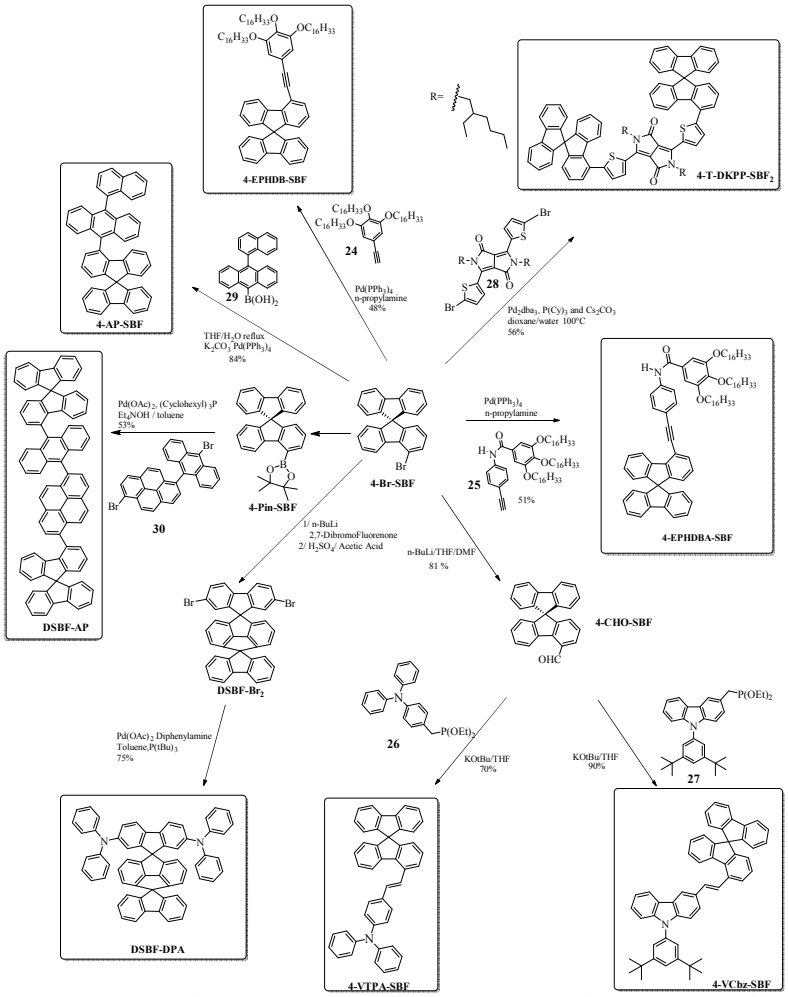

Figure 25: Synthesis of **4-EPHDB-SBF**,[94] **4-T-DKPP-SBF$_2$**,[124] **4-EPHDBA-SBF,**[94] **4-VCbz-SBF**,[126] **4-VTPA-SBF,**[126] **DSBF-DPA,**[121] **DSBF-AP**,[123] and **4-AP-SBF**[122]

4-Br-SBF platform is again the cornerstone of almost all the dyes reported in this last part (Figure 25). Thus, Camerel et al. have reported a convergent synthesis using the 4-SBF scaffold as connecting core. **4-EPHDB-SBF** and **4-EPHDBA-SBF** were synthesized in moderate yields of 48 and 51% respectively, by Sonogashira type cross-coupling reactions between **4-Br-SBF** and two different ethynyl fragments either **24** (for **4-EPHDB-SBF**) or **25** (for **4-EPHDBA-SBF**).[94] **4-T-DKPP-SBF$_2$** was synthesized by Leclerc et al. from the coupling of **4-Br-SBF** and the bis-brominated DPP-based moiety **28**. The authors report a screening of different experimental conditions (catalyst, ligand and solvent) and the best conditions found (yield 56%) involve the use of Tris(dibenzylideneacetone)dipalladium(0) (Pd_2dba_3), tricyclohexylphosphine ($P(Cy)_3$) and Cs_2CO_3 in a dioxane/water mixture at a temperature of 100°C for 24 hours.[124] A similar Suzuki coupling between **4-Br-SBF** and [10-(1-Naphthyl)-9-anthryl]boronic acid **29** gives **4-AP-SBF** with a high yield of 84%.[122] **DSBF-AP** was prepared in 53 % yield by reaction of **4-Pin-SBF** with 1-bromo-6-(9-bromo-anthracen-10-yl)-pyrene **30** in presence of $Pd(OAc)_2$, $P(Cy)_3$ and Et_4NOH in toluene.[123] Finally, the fused structure of **DSBF-DPA**[121] was synthesized from the coupling of **4-Br-SBF** with 2,7-dibromofluorenone in the presence of BuLi followed by an intramolecular cyclisation on the C5 position of the same fluorene providing the fused structure **DSBF-Br$_2$**. Incorporation of the two amines was then classically performed ($Pd(OAc)_2$, diphenylamine, $P(tBu)_3$) to give **DSBF-DPA** with 75%.
4-CHO-SBF,[126] involved in the synthesis of both **4-VTPA-SBF** and that of **4-VCbz-SBF**, was synthesized through the formylation of **4-Br-SBF** using n-BuLi and DMF in a 81 % yield. From **4-CHO-SBF** and the corresponding phosphonate derivatives (**26** or **27**), the Horner-Wadsworth-Emmons reaction produced the corresponding compounds possessing either an arylamine (**4-VTPA-SBF**, yield 70%) or N-

arylcarbazole (**4-VCbz-SBF**, yield 90%).[126] The synthesis of **4-VTPA-SBF(t-Bu)$_2$** is built on a similar strategy involving as key scaffold the 2',7'-di-tert-butyl-9,9'-spirobi[fluorene]-4-carbaldehyde.[125]

Electronic Properties

The electrochemical and optical properties of the molecules presented in this last part follow the rules detailed in the previous ones and hence will not be detailed. For example, the π-conjugation disruption between the fluorene and its C4-substituent is clearly highlighted by a blue shift in UV-Vis absorption for **4-T-DKPP-SBF$_2$**, **4-VTPA-SBF** or **4-EPHDB-SBF** compared to their C-2 isomers.[94, 124, 126] However, and oppositely to the first parts, the molecular fragments borne by the carbon in C4 such as anthracene/pyrene in **4-AP-SBF**, diketopyrrolopyrrole in **4-TDKPP-SBF$_2$** or vinyl carbazole in **4-VTPA-SBF** have high molar absorption coefficients. The resulting absorption spectra are hence strongly modified. **4-T-DKPP-SBF$_2$** provides an interesting example of such feature with strong absorptions between 300 and 650 nm.[124]

To conclude, we would like to briefly state the different applications, in which such 4-substituted SBFs have been involved. First, in fluorescent OLED either as emitter (**DSBF-AP**)[123] or as fluorescent dopant (**4-AP-SBF**,[122] **4-VTA-SBF(t-Bu)$_2$**,[125] **4-VTPA-SBF** and **4-VCbz-SBF**).[126]

With **DSBF-AP** as blue emitter in the EML, the OLED has the following architecture: ITO(100nm)/ 2-TNATA(60nm)/NPB(15nm)/ **DSBF-AP** (35nm)/Alq_3 or TPBi(20nm)/LiF(1nm)/Al(200nm). The OLEDs start to emit light at 5.13 V (with Alq_3 as ETL) or at 6.00 V (with TPBi as ETL) and reach EQE of ca 3% in both cases. The electroluminescence spectra present a maximum at 462/464 nm showing the efficiency of **DSBF-AP** as blue emitter.[123]

4-VTPA-SBF, **4-VCbz-SBF** and **4-VTA-SBF(t-Bu)$_2$** have been used as blue dopant (guest) in MADN (host). With EML: **4-VTPA-SBF** 10 wt% in MADN, a maximum EQE of 3.4%, LE of 3.9 cd/A and PE of 2.4 Lm/W and a V_{on} of 5.1 V is reported.[126] Using **4-VCbz-SBF** (EML: **4-VCbz-SBF** 10 wt% in MADN), despite a better charge injection and hence a lower V_{on} of 4.1 V, leads to a less efficient device with maximum EQE of 2.7%, LE of 2.8 cd/A and PE of 2.2 Lm/W.[126] The structurally related **4-VTPA-SBF(*t*-Bu)$_2$** used in an almost identical device (EML: **4-VTPA-SBF(*t*-Bu)$_2$** 5 wt% in MADN) leads to comparable device performance: V_{on} of 4.5 V, EQE of 2.6%, LE of 3.3 cd/A and PE of 2.1 Lm/W.[125] It should be mentioned that this performance is lower than that of its 2-substituted regioisomer also studied by the authors (EQE =3.7 %, CE = 4.5 cd/A and PE= 2.7 Lm/W).

Table 8. Selected electronical and physical data for **4-AP-SBF**,[122] **DSBF-AP**,[123] **4-EPHDBA-SBF**, **4-EPHDB-SBF**,[94] **4-VTPA-SBF, 4-VCbz-SBF**,[126] **DSBF-DPA**[121], **4-TDKPP-SBF$_2$**[124] and **4-VTPA-SBF(t-Bu)$_2$**[125]

	4-AP-SBF	DSBF-AP	4-EPHDBA-SBF	4-EPHDB-SBF	4-VTPA-SBF	4-VCbz-SBF	DSBF-DPA	4-TDKPP-SBF$_2$	4-VTPA-SBF(t-Bu)$_2$
$\lambda_{max,abs}$ (nm)	309, 342, 355, 374, 394	351,379,400[g]	309, 326, 348[f]	309,319, 341[f]	375[a]	362[a]	309, 373	530, 570	370[a]
$\lambda_{max,fluo}$ solution (nm)	403/413	443[g]	371	401	448[a]	432[a]	404	-	468[a]
$\lambda_{max,fluo}$, thin film (nm)	415 verifier	458	454	389	479	467	-	-	455
Φ_{sol} (%)[i]	-	0.83	0.006 (0.12)[j]	0.37 (0.39)[j]	0.95[b]	0.4[b]	-	-	0.65[b]
ΔE^{opt} (eV)	-	2.94	-	-	2.91	2.91	3.12	2.02	2.93
HOMO (eV)	-	-5.78[c]	-	-	-5.48[c]	-5.57[d]	-5.56[e]	-5.65	-5.59[c]
LUMO (eV)	-	-2.84[h]	-	-	-2.57[c]	-2.66[d]	-2.44[d]	-3.75	-2.66[d]

a. In DCM, b. in DCM with 4,4'-bis[4-(diphenyl-amino)styryl]biphenyl as internal reference, c. from UPS, d. from HOMO and ΔE^{opt} in solution , e. from cyclic voltammetry, f. in cyclohexane, g: in chloroform, h. LUMO=HOMO+ΔE^{opt}, i. in solution, j.in solid state

4-AP-SBF was used as a host material for the fluorescent dopant diphenyl-[4-(2-[1,1;4,1]terphenyl-4-yl-vinyl)-phenyl]-amine (BD-1). With EML: 7wt% BD-1 in **4-AP-SBF**, the authors report an OLED displaying an EQE of ca 3.4%.[122]

Finally, **DSBF-DPA** was employed as hole transporting material (HTM) in a green PhOLED (EML=$Ir(ppy)_3$) in bis-9,9'-spirobi[fluoren-2- yl]-methanone (BSFM)) and the device performance was compared to that of a similar device using NPB instead of **DSBF-DPA** as HTM.[121] The EQE obtained with the device using **DSBF-DPA** is reported at 16.5%, which is much higher than that of the device using NPB (EQE=10.4%). The authors explain such performance improvement by the E_T of **DSBF-DPA** (2.44 eV) which is higher than that of $Ir(ppy)_3$ (2.42 eV) preventing any quenching of the triplet exciton by **DSBF-DPA** (such a quenching may indeed occur using NPB as HTM, as the E_T of NPB, 2.3 eV, is lower than that of $Ir(ppy)_3$).

Another promising application has recently been reported by Leclerc et al. They have indeed reported the incorporation of a SBF core substituted in C4 (**4-T-DKPP-SBF$_2$**) as end capper in a soluble electron-donor fragment for photovoltaic applications.[124] Despite, the low OPV performances (lower than that of its C2 isomer), the authors show that the incorporation of SBF as a three-dimension platform into conjugated material backbones allows increasing the solubility despite the low density of grafted alkyl side chains and brings a more isotropic character to the charge transport properties of the final materials (hole mobilities are reported in the 6-7x10^{-5} cm^2/V.s range). The authors also show that different molecular packing can be obtained depending of the substitution pattern (C2 *vs* C4) of the SBF core.

Finally, SBF based molecules have only been recently incorporated as the central core of a mesogenic molecule.[94] The grafting of N-(ethynylphenyl) benzamide carrying hexadecyl carbon chains on a bulky dispiro[fluorene-9,11'-indeno[1,2-*b*]fluorene-12',9''-fluorene] core has for example allowed the emergence of strongly luminescent liquid crystalline phases.[127] This strategy, which consists to attach protomesogenic fragments, on a π-conjugated backbone has hence been applied by Camerel et al. on a 4-substituted SBF scaffold leading to **4-EPHDBA-SBF** and **4-EPHDB-SBF**.[94] This approach has allowed to tune the luminescence properties but also to control the self-organisation ability inside luminescent and fluid thin films. Of particular interest, **4-EPHDBA-SBF** which was poorly emissive in solution is reported to present a higher quantum yield in the solid state, highlighting the interest of the strategy described by the authors to obtain efficient blue emitters in the solid state.

Conclusion

Through a structure properties relationhip approach, the present review reports the state of the art of an emerging family of molecules, namely the 4-substituted SBFs, regarding synthesis, physico-chemical/photophysical properties and applications as host in PhOLEDs. If the substitution in position 2 of a SBF core has been widely developed to date, the substitution in position 4 is very recent (less than that 10 years) and still need to be explored. The main characteristic of this family of OSCs is the π-conjugation breaking occurring between the substituent in C4 and the fluorene backbone. This breaking of the conjugation is due to a large fluorene/substituent dihedral angle, which disrupts the electronic coupling between the two molecular fragments. Thus, as a function of the steric congestion induced by the substituent attached in C4, the intensity of the π-conjugation can be tuned. This is a key point, which will be surely developped in the future to control the intensity of the conjugation in such materials. Thanks to the spiro-bridge, excellent thermal and morphological properties are also reported for all the dyes built on a 4-substituted SBF scaffold, which are key properties for the lifetime of electronic devices. The substitution in C4 also leads to many other unusual features such as the deformation of the fluorene core or more interestingly the peculiar fluorescence emission. If the exact origin of the fluorescence emission of 4-substituted SBFs has not been yet fully understood and deserves a particular interest, some answers start to be very recently reported in the literature.[95]

The π-conjugation disruption present in 4-substituted SBF also leads to molecules possessing high triplet energy E_T. This E_T is to date the property, which has been the most used and particularly in

PhOLEDs. Thus, thanks to their high E_T, 4-substituted SBFs have been successfully introduced as host for red, green and more importantly blue PhOLEDs. Some examples of high efficiency green and blue PhOLEDs have already been published but some improvements still need to be done. For example, bipolar materials built on a 4-substituted SBF core are still very rare and in the light of literature, these molecules can lead to a strong enhancement of green and blue PhOLEDs performance.[53] Such molecules could also be used in single layer green or even blue PhOLEDs, which are also very rare in literature. In addition, recent works have also highlighted that the 4-substituted SBF can also be used for other applications than hosting phosphors in PhOLEDs. Indeed, compared to their 2-substituted analogues, different π–stacking can be obtained with 4-substituted SBF, which can lead to very different solid state properties. [94,124] This structural particularity will be surely use in the future in the field of organic solar cells and more generally in materials science.

To conclude, 4-substituted SBFs have appeared in the last years as very interesting and promising OSCs mainly to host green and blue phosphors in PhOLEDs but also very recently for other applications such as solar cells. We are convinced that these molecules can become, as their 2-substituted counterparts, an important family of OSCs for organic electronics.

Acknowledgments:

The authors would like to highly thank all their collaborators which have strongly contribute to the developments of 4-substituted SBFs in the group. They would like to highly thank Dr D. Tondelier and B. Geffroy (Paris Saclay) for the PhOLEDs fabrications and characterizations, Dr M. Romain, Dr S. Thiery, Dr O. Jeannin, Dr C. Quinton, L. Sicard (Rennes) for synthesis, physicochemical analyses, molecular modelling, and Dr E. Jacques (Rennes) for mobility measurements. They thank the CDIFX and CRMPO (Rennes), the CINES (project 2016085032, Montpellier), the ANR (HOME-OLED project n°11-BS07-020-01 and MEN IN BLUE project n°14-CE05-0024), the Région Bretagne and the ADEME (Dr B. Laffite).

ACRONYMES used in this review

2,7-Br_2-SBF: 9,9'-Spirobi[9*H*-fluorene], 2,7-dibromo-
2-DBF-SBF: 2-(9,9'-spirobi[9*H*-fluoren]-2-yl)-dibenzofuran
2-DBT-SBF: 2-(9,9'-spirobi[9*H*-fluoren]-2-yl)-dibenzothiophene
2,7-DiCbz-SBF-4'-$POPh_2$: 9,9'-(4'-diphenyl-phosphine oxide-9,9'-spirobi[9*H*-fluorene]-2,7-diyl)bis-9*H*-carbazole
2-Ph-SBF: 2-phenyl-9,9'-spirobi[fluorene]
2-$POPh_2$-SBF: diphenyl-9,9'-spirobi[9*H*-fluoren]-2-yl- phosphine oxide
2-4Py-SBF: 4-(9,9'-spirobi[fluoren]-2-yl)pyridine
2-5Pm-SBF: 5-(9,9'-spirobi[fluoren]-2-yl)pyrimidine
2,2'-$(SBF)_2$: 2,2''-Bi-9,9'-spirobi[9*H*-fluorene]
2,2'-$(SBF)_3$: 2,2'':2''',2''''-Ter-9,9'-spirobi[9*H*-fluorene]
2,7,4'-$(SBF)_3$: 2,7-di(9,9'-spirofluorenyl-4-yl)-9,9'-spirobifluorene
2,7,2'-$(SBF)_3$: 2,2'':7'',2''''-Ter-9,9'-spirobi[9*H*-fluorene]
2,7,2'-$(SBF)_4$: 2,2'':7'',2'''':7'''',2''''''-Quater-9,9'-spirobi[9*H*-fluorene]
3-$B(OH)_2$-SBF: 9,9'-spirobi[fluoren]-3-ylboronic acid
4-AP-SBF: 4-(10-(naphtalen-1-yl)anthracen-9-yl)-9,9'-spirobi[fluorene]
4-Br-SBF: 4-bromo-9,9'-spirobifluorene
4,4'-Br_2-SBF: 4,4'-dibromo-9,9'-Spirobi[9*H*-fluorene]
4-DBF-SBF: 4-(9,9'-spirobi[9*H*-fluoren]-4-yl)-dibenzofuran
4-DBT-SBF: 4-(9,9'-spirobi[9*H*-fluoren]-4-yl)-dibenzothiophene
4-EPHDB-SBF: 4-((3,4,5-tris(hexadecyloxy)phenyl)ethynyl)-9,9'-spirobi[fluorene]
4-EPHDBA-SBF: N-(4-(9,9'-spirobi[fluoren]-4-ylethynyl)phenyl)-3,4,5-tris(hexadecyloxy)benzamide
4,4'-FO-SBF: 4-(9,9'-spirobi[9*H*-fluoren]-4-yl)- 9*H*-Fluoren-9-one
4,4'-Pin_2-SBF: 4,4'-(9,9'-spirobi[9*H*-fluorene]-4,4'-diyl)bis[4,4,5,5-tetramethyl-1,3,2-Dioxaborolane]
4-Pin-SBF: 4-(9,9'-spirobi[fluoren]-4-yl)-4,4,5,5-tetramethyl-1,3,2-dioxaborolane
4-Ph-SBF: 4-phenyl-9,9'-spirobi[fluorene]
4-PhCBz-SBF: 4-N-phenyl-carbazole-9,9'-spirobi[fluorene]
4-$PhOMe_3$-SBF: 4-(3,4,5-trimethoxyphenyl)-9,9'-spirobi[fluorene]
4-$POPh_2$-SBF: diphenyl-9,9'-spirobi[9*H*-fluoren]-4-yl-Phosphine oxide
4-4Py-SBF: 4-(9,9'-spirobi[fluoren]-4-yl)pyridine
4-3Py-SBF: 3-(9,9'-spirobi[fluoren]-4-yl)pyridine
4-2Py-SBF: 2-(9,9'-spirobi[fluoren]-4-yl)pyridine
4-5Pm-SBF: 5-(9,9'-spirobi[fluoren]-4-yl)pyrimidine
4-SFA-SFA: 10,10'-diphenyl-4',4''-bispiro[acridine-9(10*H*),9'-[9*H*]fluorene]

4-SFA-SBF: 10-phenyl-4'-(9,9'-spirobi[9*H*-fluoren]-4-yl)-spiro[acridine-9(10*H*),9'-[9*H*]fluorene]
4,4'-(SBF)$_2$: 4-(9,9'-spirofluorenyl-4-yl)-9,9'-spirobifluorene
4,3'-(SBF)$_2$: 3,4'-Bi-9,9'-spirobi[9*H*-fluorene]
4,4'-(SBF)$_3$: 4,4'':4''',4'''':Ter-9,9'-spirobi[9*H*-fluorene]
4,4'-(SBF)$_4$: 4,4'':4''',4'''':4''''',4'''''':Quater-9,9'-spirobi[9*H*-fluorene]
4,4'-(SBF)$_5$: 4,4'':4''',4'''':4''''',4'''''':4'''''',4''''''':Quinque-9,9'-spirobi[9*H*-fluorene]
4-T-DKPP-SBF$_2$: 3,6-bis(5-(9,9'-spirobi[fluoren]-5-yl)thiophen-2-yl)-2,5-bis(2-ethylhexyl)pyrrolo[3,4-*c*]pyrrole-1,4(2*H*,5*H*)-dione
4-VCbz-SBF: (*E*)-3-(2-(9,9'-spirobi[fluoren]-4-yl)vinyl)-9-(3,5-di-tert-butylphenyl)-9H-carbazole
4-VTPA-SBF: (*E*)-4-(2-(9,9'-spirobi[fluoren]-4-yl)vinyl)-N,N-diphenylaniline
4-VTPA-SBF(t-Bu)$_2$: (*E*)-4-(2-(2',7'-di-tert-butyl-9,9'-spirobi[fluoren]-4-yl)vinyl)-N,N-diphenylaniline
AcOH: acetic acid
Alq3: tris(8-hydroxyquinoline)aluminum
BCP: 2,9-dimethyl-4,7-diphenyl-1,10-phenanthroline
BD-1: diphenyl-[4-(2-[1,1';4',1"]terphenyl-4-yl-vinyl)-phenyl]-amine
BSFM : bis-9,9'-spirobi[fluoren-2- yl]-methanone
(Btp)$_2$Ir(acac): bis[2-(20-benzo[4,5-a]thienyl)pyridinato-N,C30] iridium(acetylacetonate)
CE: Current efficiency (in OLED or PhOLED)
ClPPh$_2$: chlorodiphenylphosphine
CuPc: copper phthalocyanine
DCM: dichloromethane
ΔE^{el}: electrochemical band gap
ΔE^{opt}: optical energy gap
DMF: *N,N*-Dimethylformamide
DNTPD: N,N'-diphenyl-N,N'-bis-[4-(phenyl-*m*-tolyl-amino)-phenyl]-biphenyl-4,4'-diamine
DSBF-DPA: N,N,N',N'-tetraphenyl-spiro(cyclopenta[de]fluorene-1,5,9',9''-bifluorene)-2',7'-diamine
DSF[2,1-*c*]IF: dispiro[fluorene-9,5'-indeno[2,1-c]fluorene-8',9''-fluorene]
DSBF-AP: 1-spiro-9,9'-bifluoren-4-yl-6-(10-spiro-9,9'-bifluoren-4-yl-anthracen-9-yl)-pyrene
DSC: differential scanning calorimetry
EML: emitting layer (in OLED or PhOLED)
EQE: external quantum efficiency (in OLED or PhOLED)
E_T: triplet energy
FIrpic: Bis[2-(4,6-difluorophenyl)pyridinato-C^2,*N*](picolinato)iridium(III)
HAT-CN: Dipyrazino[2,3-f:2',3'-h]quinoxaline 2,3,6,7,10,11-hexacarbonitrile
HOMO: Highest Occupied Molecular Orbital
HTM: Hole Transporting Material
Ir(ppy)$_2$acac: Bis[2-(2-pyridinyl-*N*)phenyl-C](2,4-pentanedionato-O^2,O^4)iridium(III)
Ir(ppy)$_3$: Tris[2-phenylpyridinato-C^2,*N*]iridium(III)
ITO: Indium-Tin oxide
K$_2$CO$_3$: potassium carbonate
k_{nr}: non radiative rate constant
k_r: radiative rate constant
LiF: Lithium fluoride
Liq: 8-Hydroxyquinolinolato-lithium
LUMO: Lowest Unoccupied Molecular Orbital
MADN: 2-methyl-9,10-di(2-naphthyl)anthracene
mCP: *N,N'*-dicarbazolyl-3,5-benzene
2-Me-THF: 2-Methyltetrahydrofuran
MoO$_3$: Molybdenum trioxide
NPB: N'-di(1-naphtyl)-N,N'-diphenylbenzidine
MsOH: methanesulfonic acid
n-BuLi: n-Butyllithium
OLED: organic light-emitting diode
OSC: Organic Semi-Conductor
P(Cy)$_3$: Tricyclohexylphosphine
Pd$_2$dba$_3$: Tris(dibenzylideneacetone)dipalladium(0)
Pd(dppf)Cl$_2$: [1,1'-Bis(diphenylphosphino)ferrocene]dichloropalladium(II)
Pd(OAc)$_2$: Palladium(II) acetate
Pd(PPh$_3$)$_4$: Tetrakis(triphenylphosphine)palladium(0)
PE: power efficiency (in OLED or PhOLED)
PEDOT-PSS: polyethylenedioxythiophene-polystyrene sulfonate
PHC: pure hydrocarbon
Ph$_2$Br: 2-bromo-biphenyl
PhOLED: phosphorescent organic ligth-emitting diode
(ppq)$_2$Ir(acac): bis(2,4-diphenylquinolyl-N,C2')iridium(acetylacetonate)
Φ_{sol}: quantum yield
rt: room temperature
SBF: 9,9'-spirobifluorene
SBF: spirobifluorene
Spiro-2CBP: 2,7-Bis(carbazol-9-yl)-9,9-spirobifluorene
Spiro-OMeTAD : 2,2',7,7'-Tetrakis[N,N-di(4-methoxyphenyl)amino]-9,9'-spirobifluorene
TAPC: Di-[4-(N,N-di-*p*-tolyl-amino)-phenyl]cyclohexane

T_d: decomposition temperature
T_g: glass transition temperature
TGA: thermogravimetric analysis
TCTA: Tris(4-carbazoyl-9-ylphenyl)amine
THF: tetrahydrofuran
TMEDA: Tetramethylethylenediamine
TmPyPB: 1,3,5-Tri[(3-pyridyl)-phen-3-yl]benzene
TPBi: 2,2',2''-(1,3,5-Benzinetriyl)-tris(1-phenyl-1-*H*-benzimidazole)
V_{on}: threshold voltage (in OLED or PhOLED)

REFERENCES

1 L.-H. Xie, J. Liang, J. Song, C.-R. Yin and W. Huang, *Current Organic Chemistry*, 2010, **14**, 2169.
2 T. P. I. Saragi, T. Spehr, A. Siebert, T. Fuhrmann-Lieker and J. Salbeck, *Chem. Rev.*, 2007, **107**, 1011.
3 M. Romain, S. Thiery, A. Shirinskaya, C. Declairieux, D. Tondelier, B. Geffroy, O. Jeannin, J. Rault-Berthelot, R. Métivier and C. Poriel, *Angew. Chem. Int. Ed.*, 2015, **54**, 1176.
4 M. Romain, D. Tondelier, J.-C. Vanel, B. Geffroy, O. Jeannin, J. Rault-Berthelot, R. Métivier and C. Poriel, *Angew. Chem. Int. Ed.*, 2013, **52**, 14147.
5 R. Mertens, *The OLED Handbook: A Guide to OLED Technology, Industry & Market*, 2012 edition, 2012.
6 R. S. Sanchez and E. Mas-Marza, *Solar Energy Materials and Solar Cells*, 2016, **158, Part 2**, 189.
7 N.-G. Park, *Materials Today*, 2015, **18**, 65.
8 D. Thirion, C. Poriel, R. Métivier, J. Rault-Berthelot, F. Barrière and O. Jeannin, *Chem. Eur. J.*, 2011, **17**, 10272.
9 C. Poriel, J. Rault-Berthelot, D. Thirion, F. Barrière and L. Vignau, *Chem. Eur. J.*, 2011, **17**, 14031.
10 D. Horhant, J.-J. Liang, M. Virboul, C. Poriel, G. Alcaraz and J. Rault-Berthelot, *Org. Lett.*, 2006, **8**, 257.
11 C. Poriel, J. Rault-Berthelot, F. Barrière and A. M. Z. Slawin, *Org. Lett.*, 2008, **10**, 373.
12 D. Thirion, M. Romain, J. Rault-Berthelot and C. Poriel, *J. Mater. Chem.*, 2012, **22**, 7149.
13 L.-H. Xie, X.-Y. Hou, C. Tang, Y.-R. Hua, R.-J. Wang, R.-F. Chen, Q.-L. Fan, L.-H. Wang, W. Wei, B. Peng and W. Huang, *Org. Lett.*, 2006, **8**, 1363.
14 F. Barrière, C. Poriel and J. Rault-Berthelot, *Electrochim. Acta*, 2013, **110**, 735.
15 C. Poriel, F. Barrière, D. Thirion and J. Rault-Berthelot, *Chem. Eur. J.*, 2009, **15**, 13304.
16 J.-H. Xie and Q.-L. Zhou, *Acc. Chem. Res.*, 2008, **41**, 581.
17 C. Poriel, Y. Ferrand, P. Le Maux, J. Rault-Berthelot and G. Simonneaux, *Synth. Met.*, 2008, **158**, 796.
18 X. Cheng, Q. Zhang, J.-H. Xie, L.-X. Wang and Q.-L. Zhou, *Angew. Chem. Int. Ed.*, 2005, **44**, 1118.
19 X. Cheng, S.-F. Zhu, X.-C. Qiao, P.-C. Yan and Q.-L. Zhou, *Tetrahedron*, 2006, **62**, 8077.
20 D. Lorcy, L. Mattiello, C. Poriel and J. Rault-Berthelot, *J. Electroanal. Chem.*, 2002, **530**, 33.
21 C. Poriel, Y. Ferrand, P. Le Maux, C. Paul-Roth, G. Simonneaux and J. Rault-Berthelot, *J. Electroanal. Chem.*, 2005, **583**, 92.
22 Y. Ferrand, C. Poriel, P. Le Maux, J. Rault-Berthelot and G. Simonneaux, *Tetrahedron Asymmetry*, 2005, **16**, 1463.
23 C. Poriel, Y. Ferrand, P. Le Maux, J. Rault-Berthelot and G. Simonneaux, *Inorg. Chem.*, 2004, **43**, 5086.
24 C. Poriel, Y. Ferrand, P. Le Maux, J. Rault-Berthelot and G. Simonneaux, *Chem. Commun.*, 2003, 1104.
25 C. Poriel, Y. Ferrand, P. Le Maux, C. Paul, J. Rault-Berthelot and G. Simonneaux, *Chem. Commun.*, 2003, 2308.
26 C. Paul-Roth, J. Rault-Berthelot, G. Simonneaux, C. Poriel, M. Abdalilah and J. Letessier, *J. Electroanal. Chem.*, 2006, **597**, 19.
27 C. Poriel, Y. Ferrand, P. Le Maux, J. Rault-Berthelot and G. Simonneaux, *Tetrahedron Lett.*, 2003, **44**, 1759.
28 C. Poriel, Y. Ferrand, S. Juillard, P. Le Maux and G. Simonneaux, *Tetrahedron*, 2004, **60**, 145.
29 C. Poriel, Y. Ferrand, P. Le Maux and G. Simonneaux, *Synlett.*, 2003, 71.
30 F. Moreau, N. Audebrand, C. Poriel, V. Moizan-Baslé and J. Ouvry, *J. Mater. Chem.*, 2011, **21**, 18715.
31 H.-D. Guo, X. M. Guo, S. R. Batten, J.-F. Song, S.-Y. Song, S. Dang, G.-L. Zheng, J.-K. Tang and H.-J. Zhang, *Cryst. Growth Des.*, 2009, **9**, 1394.
32 K.-T. Wong, Y.-L. Liao, Y.-C. Peng, C.-C. Wang, S.-Y. Lin, C.-H. Yang, S.-M. Tseng, G.-H. Lee and S.-M. Peng, *Cryst. Growth Des.*, 2005, **5**, 667.
33 C. Poriel, R. Métivier, J. Rault-Berthelot, D. Thirion, F. Barrière and O. Jeannin, *Chem. Commun.*, 2011, **47**, 11703.
34 N. Fomina, S. E. Bradforth and T. E. Hogen-Esch, *Macromolecules*, 2009, **42**, 6440.
35 S. Y. Hong, D. Y. Kim, C. Y. Kim and R. Hoffmann, *Macromolecules*, 2001, **34**, 6474.
36 P. Guiglion and M. A. Zwijnenburg, *Phys. Chem. Chem. Phys.*, 2015, **17**, 17854.
37 S. Karaburnaliev, M. Baumgarten, N. Tyutyulkov and K. Müllen, *J. Phys. Chem.*, 1994, **98**, 11892.
38 C.-W. Lee and Y. Lee, *Chem. Mater.*, 2014, **26**, 1616.

39 B. Pan, B. Wang, Y. Wang, P. Xu, L. Wang, J. Chen and D. Ma, *J. Mater. Chem. C*, 2014, **2**, 2466.
40 S. Gong, Y.-L. Chang, K. Wu, R. White, Z.-H. Lu, D. Song and C. Yang, *Chem. Mater.*, 2014, **26**, 1463.
41 L.-S. Cui, S.-C. Dong, Y. Liu, M.-F. Xu, Q. Li, Z.-Q. Jiang and L.-S. Liao, *Org. Electron.*, 2013, **14**, 1924.
42 Y. Liu, L.-S. Cui, X.-B. Shi, Q. Li, Z.-Q. Jiang and L.-S. Liao, *J. Mater. Chem. C*, 2014, **2**, 8736.
43 Y.-M. Xie, L.-S. Cui, F.-S. Zu, F. Igbari, M.-M. Xue, Z.-Q. Jiang and L.-S. Liao, *Org. Electron.*, 2015, **26**, 25.
44 H. Sasabe and J. Kido, *Chem. Mater.*, 2011, **23**, 621.
45 M.-K. Leung, W.-H. Yang, C.-N. Chuang, J.-H. Lee, C.-F. Lin, M.-J. Wei and Y.-H. Liu, *Org. Lett.*, 2012, **14**, 4986.
46 C. Fan, Y. Chen, Z. Liu, Z. Jiang, C. Zhong, D. Ma, J. Qin and C. Yang, *J. Mater. Chem. C*, 2013, **1**, 463.
47 K. S. Yook and J. Y. Lee, *Adv. Mater.*, 2012, **24**, 3169.
48 S. Gong, Q. Fu, W. Zeng, C. Zhong, C. Yang, D. Ma and J. Qin, *Chem. Mater.*, 2012, **24**, 3120.
49 Q. Bai, H. Liu, L. Yao, T. Shan, J. Li, Y. Gao, Z. Zhang, Y. Liu, P. Lu, B. Yang and Y. Ma, *ACS Appl. Mater. Interfaces*, 2016, **8**, 24793.
50 J. Zhao, G.-H. Xie, C.-R. Yin, L.-H. Xie, C.-M. Han, R.-F. Chen, H. Xu, M.-D. Yi, Z.-P. Deng, Chen, Shu-Fen, S.-Y. Liu and W. Huang, *Chem. Mater.*, 2011, **23**, 5331.
51 C. Han, Z. Zhang, H. Xu, G.-H. Xie, R. Chen, Y. Zhao and W. Huang, *Angew. Chem. Int. Ed.*, 2012, **51**, 10104.
52 F. May, M. Al-Hewi, B. Baumeier, W. Kowalsky, E. Fuchs, C. Lennartz and D. Andrienko, *J. Am. Chem. Soc.*, 2012, **134**.
53 S. Thiery, D. Tondelier, B. Geffroy, E. Jacques, M. Robin, R. Métivier, O. Jeannin, J. Rault-Berthelot and C. Poriel, *Org. Lett.*, 2015, **17**, 4682.
54 C.-J. Lin, H.-L. Huang, M.-R. Tseng and C.-H. Cheng, *J. Display. Tech.*, 2009, **5**, 236.
55 Y.-X. Zhang, L. Zhang, L.-S. Cui, C.-H. Gao, H. Chen, Q. Li, Z.-Q. Jiang and L.-S. Liao, *Org. Lett.*, 2014, **16**, 3748.
56 L. Ding, S.-C. Dong, Z.-Q. Jiang, H. Chen and L. S. Liao, *Adv. Funct. Mat.*, 2015, **25**, 645.
57 H. N. Ohkuma, T., K. Shizu, T. Yasuda and C. Adachi, *Chem. Lett.*, 2014, **43**, 1017.
58 K. Nasu, T. Nakagawa, H. Nomura, C.-J. Lin, C.-H. Cheng, M.-R. Tseng, T. Yasuda and C. Adachi, *Chem. Commun.*, 2013, **49**, 10385.
59 M. Romain, D. Tondelier, B. Geffroy, O. Jeannin, E. Jacques, J. Rault-Berthelot and C. Poriel, *Chem. Eur. J.*, 2015, **21**, 9426.
60 M. Romain, D. Tondelier, B. Geffroy, A. Shirinskaya, O. Jeannin, J. Rault-Berthelot and C. Poriel, *Chem. Commun.*, 2015, **51**, 1313.
61 M. Romain, D. Tondelier, O. Jeannin, B. Geffroy, J. Rault-Berthelot and C. Poriel, *J. Mater. Chem. C*, 2015, **3**, 9701.
62 C. Poriel, J. Rault-Berthelot, C. Quinton, S. Thiery, B. Geffroy, D. Tondelier and R. Métivier, *Chem. Eur. J.*, 2016, **22**, 17930.
63 S. Thiery, D. Tondelier, B. Geffroy, O. Jeannin, J. Rault-Berthelot and C. Poriel, *Chem. Eur. J.*, 2016, **22**, 10136.
64 C. Fan, L. Zhu, T. Liu, B. Jiang, D. Ma, J. Qin and C. Yang, *Angew. Chem. Int. Ed.*, 2014, **53**, 2147.
65 M.-K. Leung, Y.-H. Hsieh, T.-Y. Kuo, P.-T. Chou, J.-H. Lee, T.-L. Chiu and H.-J. Chen, *Org. Lett.*, 2013, **15**, 4694.
66 Y. Zheng, A. S. Batsanov, V. Jankus, F. B. Dias, M. R. Bryce and A. P. Monkman, *J. Org. Chem.*, 2011, **76**, 8300.
67 T.-L. Chiu, H.-J. Chen, Y.-H. Hsieh, J.-J. Huang and M.-k. Leung, *J. Phys. Chem. C*, 2015, **119**, 16846.
68 J.-J. Huang, Y.-H. Hung, P.-L. Ting, Y.-N. Tsai, H.-J. Gao, T.-L. Chiu, J.-H. Lee, C.-L. Chen, P.-T. Chou and M.-k. Leung, *Org. Lett.*, 2016, **18**, 672.
69 C. Fan, Y. Chen, P. Gan, C. Yang, C. Zhong, J. Qin and D. Ma, *Org. Lett.*, 2010, **12**, 5648.
70 Z. Jiang, H. Yao, Z. Zhang, C. Yang, Z. Liu, Y. Tao, J. Qin and D. Ma, *Org. Lett.*, 2009, **11**, 2607.
71 S. Thiery, D. Tondelier, C. Declairieux, B. Geffroy, O. Jeannin, R. Métivier, J. Rault-Berthelot and C. Poriel, *J. Phys. Chem. C*, 2015, **119**, 5790.
72 R. G. Clarkson and M. Gomberg, *J. Am. Chem. Soc.*, 1930, **52**, 2881.
73 M. Romain, M. Chevrier, S. Bebiche, T. Mohammed-Brahim, J. Rault-Berthelot, E. Jacques and C. Poriel, *J. Mater. Chem. C*, 2015, **3**, 5742.
74 E. Jacques, M. Romain, A. Yassin, S. Bebiche, M. Harnois, T. Mohammed-Brahim, J. Rault-Berthelot and C. Poriel, *J. Mater. Chem. C*, 2014, **2**, 3292.
75 C. Poriel, N. Cocherel, J. Rault-Berthelot, L. Vignau and O. Jeannin, *Chem. Eur. J.*, 2011, **17**, 12631.
76 N. Cocherel, C. Poriel, L. Vignau, J.-F. Bergamini and J. Rault-Berthelot, *Org. Lett.*, 2010, **12**, 452.
77 M. Romain, C. Quinton, D. Tondelier, B. Geffroy, O. Jeannin, J. Rault-Berthelot and C. Poriel, *J. Mater. Chem. C*, 2016, **4**, 1692.
78 C. S. Hartley, *J. Org. Chem.*, 2011, **76**, 9188.
79 C. S. Hartley, *Acc. Chem. Res.*, 2016, **49**, 646.
80 H. Yersin, *Highly Efficient OLEDs with Phosphorescent Materials*, Wiley-VCH:Verlag GMbH & Co. KGaA, Weinheim, 2007.

81 S. Thiery, D. Tondelier, C. Declairieux, G. Seo, B. Geffroy, O. Jeannin, J. Rault-Berthelot, R. Métivier and C. Poriel, *J. Mater. Chem. C*, 2014, **2**, 4156.
82 S. Thiery, C. Declairieux, D. Tondelier, G. Seo, B. Geffroy, O. Jeannin, R. Métivier, J. Rault-Berthelot and C. Poriel, *Tetrahedron*, 2014, **70**, 6337.
83 D. Thirion, C. Poriel, F. Barrière, R. Métivier, O. Jeannin and J. Rault-Berthelot, *Org. Lett.*, 2009, **11**, 4794.
84 H. Schenk, *Acta Cryst. B*, 1972, **28**, 625.
85 C.-C. Lai, M.-J. Huang, H.-H. Chou, C.-Y. Liao, P. Rajamalli and C.-H. Cheng, *Adv. Funct. Mat.*, 2015, **25**, 5548.
86 G. Méhes, H. Nomura, W. Zhang, T. Nakagawa and C. Adachi, *Angew. Chem. Int. Ed.*, 2012, **51**, 11311.
87 N. Lin, J. Qiao, L. Duan, L. Wang and Y. Qiu, *J. Phys. Chem. C*, 2014, **118**, 7569.
88 L.-S. Cui, Y.-M. Xie, Y.-K. Wang, C. Zhong, Y.-L. Deng, X.-Y. Liu, Z.-Q. Jiang and L.-S. Liao, *Adv. Mater.*, 2015, **27**, 4213.
89 K.-T. Wong, Y.-L. Liao, Y.-T. Lin, H.-C. Su and C.-C. Wu, *Org. Lett.*, 2005, **7**, 5131.
90 C.-C. Wu, T.-L. Liu, Y.-T. Lin, W.-Y. Hung, T.-H. Ke, K.-T. Wong and T.-C. Chao, *App. Phys. Lett.*, 2004, **85**, 1172.
91 C. Poriel, J.-J. Liang, J. Rault-Berthelot, F. Barrière, N. Cocherel, A. M. Z. Slawin, D. Horhant, M. Virboul, G. Alcaraz, N. Audebrand, L. Vignau, N. Huby, G. Wantz and L. Hirsch, *Chem. Eur. J.*, 2007, **13**, 10055.
92 M. Belletête, M. Ranger, S. Beaupré, M. Leclerc and G. Durocher, *Chem. Phys. Lett.*, 2000, **316**, 101.
93 J.-F. Wang, J.-K. Feng, A.-M. Ren and L. Yang, *Chin. J. Chem.*, 2005, **23**, 1618.
94 S. Thiery, B. Heinrich, B. Donnio, C. Poriel and F. Camerel, *J. Phys. Chem. C*, 2015, **119**, 10564.
95 C. Quinton, S. Thiery, O. Jeannin, D. Tondelier, B. Geffroy, E. Jacques, J. Rault-Berthelot and C. Poriel, *ACS Appl. Mater. Interfaces.*, 2017, **9**, 6194.
96 M. A. Baldo, D. F. O'Brien, M. E. Thompson and S. R. Forrest, *Phys. Rev. B J1 - PRB*, 1999, **60**, 14422.
97 M. A. Baldo, D. F. O'Brien, Y. You, A. Shoustikov, S. Sibley, M. E. Thompson and S. R. Forrest, *Nature*, 1998, **395**, 151.
98 D. Geuenich, K. Hess, F. Köhler and R. Herges, *Chem. Rev.*, 2005, **105**, 3758.
99 S. M. King, S. I. Hintschich, D. Dai, C. Rothe and A. P. Monkman, *J. Phys. Chem. C*, 2007, **111**, 18759.
100 N. Cocherel, C. Poriel, O. Jeannin, A. Yassin and J. Rault-Berthelot, *Dyes Pigm.*, 2009, **83**, 339.
101 A. Schweig, U. Weidner, R. K. Hill and D. A. Cullison, *J. Am. Chem. Soc.*, 1973, **95**, 5426.
102 N. Johansson, D. A. dos Santos, S. Guo, J. Cornil, M. Fahlman, J. Salbeck, H. Schenk, H. Arwin, J.-L. Bredas and W. R. Salaneck, *J. Chem. Phys.*, 1997, **107**, 2542.
103 X. Zhou, J. He, L. S. Liao, M. Lu, X. M. Ding, X. Y. Hou, X. M. Zhang, X. Q. He and S.-T. Lee, *Adv. Mater.*, 2000, **12**, 265.
104 R. Pudzich, T. Fuhrmann-Lieker and J. Salbeck, *Adv. Polym. Sci.*, 2006, **199**, 83.
105 J. Salbeck, N. Yu, J. Bauer, F. Weissörtel and H. Bestgen, *Synth. Met.*, 1997, **91**, 209.
106 K. Naito, *Chem. Mater.*, 1994, **6**, 2343.
107 E. Baranoff and B. F. E. Curchod, *Dalton Trans.*, 2015, **44**, 8318.
108 Y. Tao, L. Ao, Q. Wang, C. Zhong, C. Yang, J. QIn and D. Ma, *Chem. Asian. J.*, 2010, **5**, 278.
109 K. E. Linton, A. L. Fischer, C. Pearson, M. A. P. Fox, L.-O. Palsson, M. R. Bryce and M. C. Petty, *J. Mater. Chem.*, 2012, **22**, 11816.
110 S. O. Jeon, K. S. Yook, C. W. Joo, H. S. Son and J. Y. Lee, *Thin Solid Films*, 2010, **518**, 3716.
111 Y. Jahng and F. M. M. Rahman, *Bull. Chem. Soc. Jpn.*, 2010, **83**, 672.
112 L. Ying, J. Zou, W. Yang, A. Zhang, Z. Wu, W. Zhao and Y. Cao, *Dyes Pigm.*, 2009, **82**, 251.
113 C.-C. Wu, Y.-T. Lin, H.-H. Chiang, T. Y. Cho, C. W. Chen, K.-T. Wong, Y.-L. Liao, G.-H. Lee and S.-M. Peng, *App. Phys. Lett.*, 2002, **81**, 577.
114 R.-H. Lee, Y.-W. Huang, Y.-Y. Wang and H.-Y. Chang, *Thin Solid Films*, 2008, **516**, 5062.
115 P.-T. Wu, F. S. Kim, R. D. Champion and S. A. Jenekhe, *Macromolecules*, 2008, **41**, 7021.
116 S. E. Jang, C. W. Joo, S. O. Jeon, K. S. Yook and J. Y. Lee, *Org. Electron.*, 2010, **11**, 1059.
117 H. Nakanotani, S. Akiyama, D. Ohnishi, M. Moriwake, M. Yahiro, T. Yoshihara, S. Tobita and C. Adachi, *Adv. Funct. Mat.*, 2007, **17**, 2328.
118 S.-C. Dong, C.-H. Gao, Z.-H. Zhang, Z.-Q. Jiang, S.-T. Lee and L. S. Liao, *Phys. Chem. Chem. Phys.*, 2012, **14**, 14224.
119 S.-C. Dong, C.-H. Gao, X. D. Yuan, L.-S. Cui, Z.-Q. Jiang, S.-T. Lee and L. S. Liao, *Org. Electron.*, 2013, **14**, 902.
120 T. Liu, H. Sun, C. Fan, D. Ma, C. Zhong and C. Yang, *Org. Electron.*, 2014, **15**, 3568.
121 Y. J. Cho, O. y. Kinm and J. Y. Lee, *Org. Electron.*, 2012, **13**, 351.
122 S. E. Jang, C. W. Joo, K. S. Yook, J.-W. Kim, C.-W. Lee and J. Y. Lee, *Synth. Met.*, 2010, **160**, 1184.
123 S. Lee, B. Kim, H. Jung, H. Shin, H. Lee, J. Lee and J. Park, *Dyes Pigm.*, 2017, **136**, 255.
124 I. Bulut, P. Chavez, S. Fall, S. Mery, B. Heinrich, J. Rault-Berthelot, C. Poriel, P. Leveque and N. Leclerc, *RSC Adv.*, 2016, **6**, 25952.

125 K. H. Lee, S. O. Kim, J. N. You, S. Kang, J. Y. Lee, K. S. Yook, S. O. Jeon, J. Y. Lee and S. S. Yoon, *J. Mater. Chem.*, 2012, **22**, 5145.
126 K. H. Lee, S. O. Kim, K. S. Yook, S. O. Jeon, J. Y. Lee and S. S. Yoon, *Synth. Met.*, 2011, **161**, 2024.
127 S. Thiery, B. Heinrich, B. Donnio, C. Poriel and F. Camerel, *J. Mater. Chem. C*, 2014, **2**, 4265.